Phylogenetic relationships in the southern African genus *Drosanthemum* (Ruschioideae, Aizoaceae)

Sigrid Liede-Schumann [Corresp., 1], **Guido W Grimm** [2], **Nicolai M Nuerk** [1], **Alastair J Potts** [3], **Ulrich Meve** [1], **Heidrun EK Hartmann** [4]

1 Department of Plant Systematics, University of Bayreuth, Bayreuth, Germany

2 unaffiliated, Orléans, France

3 African Centre for Coastal Palaeoscience, Nelson Mandela University, Port Elizabeth, Eastern Cape, South Africa

4 Department of Systematics and Evolution of Plants, University of Hamburg, Hamburg, Germany

Corresponding Author: Sigrid Liede-Schumann
Email address: sigrid.liede@uni-bayreuth.de

Background. *Drosanthemum,* the only genus of the tribe Drosanthemeae, is widespread over the Greater Cape Floristic Region in southern Africa. With 114 recognized species, *Drosanthemum,* together with the highly succulent and species-rich tribe Ruschieae, constitute the 'core ruschioids' in Aizoaceae. Within *Drosanthemum*, nine subgenera have been described based on flower and fruit morphology. Their phylogenetic relationships, however, have not yet been investigated, hampering understanding of monophyletic entities and patterns of geographic distribution. **Methods**. Using chloroplast and nuclear DNA sequence data, we performed network- and tree-based phylogenetic analyses of 73 species of *Drosanthemum* with multiple accessions for widespread species. A well-curated, geo-referenced occurrence dataset comprising the 134 genetically analysed and 863 further accessions was used to describe the distributional ranges of intrageneric lineages and the genus as a whole. **Results.** Phylogenetic inference supports nine clades within *Drosanthemum*, seven of which group in two major clades, while the remaining two show ambiguous affinities. The nine clades are generally congruent to previously described subgenera within *Drosanthemum*, with exceptions such as cryptic species. In-depth analyses of sequence patterns in each gene region were used to reveal phylogenetic affinities inside the retrieved clades in more detail. We observe a complex distribution pattern including widespread, species-rich clades expanding into arid habitats of the interior (subgenera *Drosanthemum* p.p., *Vespertina*, *Xamera*) that are genetically and morphologically diverse. In contrast, less species-rich, genetically less divergent, and morphologically unique lineages are restricted to the central Cape region and more mesic conditions (*Decidua*, *Necopina*, *Ossicula*, *Quastea*, *Quadrata*, *Speciosa*). Our results suggest that the main lineages arose from an initial rapid radiation, with subsequent diversification in some clades.

1 **Phylogenetic relationships in the southern African genus**

2 ***Drosanthemum* (Ruschioideae, Aizoaceae)**

3 Sigrid Liede-Schumann[1], Guido W. Grimm[2], Nicolai M. Nürk[1], Alastair J. Potts[2], Ulrich Meve[1], Heidrun E.K.

4 Hartmann[4]

5 [1] Department of Plant Systematics, University of Bayreuth, Bayreuth, Bavaria, Germany

6 [2] unaffiliated, Orléans, France

7 [3] African Centre for Coastal Palaeoscience, Nelson Mandela University, Port Elizabeth, Eastern Cape,

8 South Africa

9 [4] formerly Department of Systematics and Evolution of Plants, University of Hamburg, Hamburg,

10 Germany; † 11 July 2016

12 Corresponding author:

13 Sigrid Liede-Schumann

14 Universitätsstrasse 30, 95440 Bayreuth, Bavaria, Germany

15 Email address: sigrid.liede@uni-bayreuth.de

Abstract

Background. *Drosanthemum,* the only genus of the tribe Drosanthemeae, is widespread over the Greater Cape Floristic Region in southern Africa. With 114 recognized species, *Drosanthemum,* together with the highly succulent and species-rich tribe Ruschieae, constitute the 'core ruschioids' in Aizoaceae. Within *Drosanthemum*, nine subgenera have been described based on flower and fruit morphology. Their phylogenetic relationships, however, have not yet been investigated, hampering understanding of monophyletic entities and patterns of geographic distribution.

Methods. Using chloroplast and nuclear DNA sequence data, we performed network- and tree-based phylogenetic analyses of 73 species of *Drosanthemum* with multiple accessions for widespread species. A well-curated, geo-referenced occurrence dataset comprising the 134 genetically analysed and 863 further accessions was used to describe the distributional ranges of intrageneric lineages and the genus as a whole.

Results. Phylogenetic inference supports nine clades within *Drosanthemum*, seven of which group in two major clades, while the remaining two show ambiguous affinities. The nine clades are generally congruent to previously described subgenera within *Drosanthemum*, with exceptions such as cryptic species. In-depth analyses of sequence patterns in each gene region were used to reveal phylogenetic affinities inside the retrieved clades in more detail. We observe a complex distribution pattern including widespread, species-rich clades expanding into arid habitats of the interior (subgenera *Drosanthemum* p.p.*, Vespertina, Xamera*) that are genetically and morphologically diverse. In contrast, less species-rich, genetically less divergent, and morphologically unique lineages are restricted to the central Cape region and more mesic conditions (*Decidua*, *Necopina*, *Ossicula*, *Quastea*, *Quadrata*, *Speciosa*). Our results suggest that the main lineages arose from an initial rapid radiation, with subsequent diversification in some clades.

Introduction

In the south-western corner of Africa, the iconic leaf-succulent Aizoaceae (ice plant family, including *Lithops*, 'living stones'; Caryophyllales) is one of the most species-rich families in the

47   biodiversity hot-spot of the Greater Cape Floristic Region (GCFR; Born, Linder & Desmet 2007;

48   Mittermeier et al. 1998, 2004, 2011), ranking second in the number of endemic genera and fifth

49   in the number of species (Manning & Goldblatt 2012). Although Aizoaceae species have

50   received much attention both in terms of their ecology and evolution (e.g., Klak, Reeves &

51   Hedderson 2004; Valente et al. 2014; Ellis, Weis & Gaut 2007; Hartmann 2006; Schmiedel &

52   Jürgens 2004, Powell et al. 2019), information on phylogenetic relationships within major clades

53   (or subfamilies) is still far from complete. Here, we aim at filling some of the knowledge-gaps

54   by: (1) providing a review of the current classification of the family, and origin and distribution

55   of major clades (in the Introduction), and (2) a study of phylogenetic relationships in the

56   enigmatic and hitherto, phylogenetically, almost neglected genus *Drosanthemum*.

57   **Subfamilies of Aizoaceae: relationship of major clades**

58   Aizoaceae currently comprises ca. 1800 species (Hartmann 2017a; Klak, Hanáček & Bruyns

59   2017a) classified in 145 genera and five subfamilies (Klak, Hanáček & Bruyns 2017a). The first

60   three subfamilies – Sesuvioideae, Aizooideae, Acrosanthoideae – are successive sisters to

61   Mesembryanthemoideae + Ruschioideae (Klak et al. 2003; Klak, Reeves & Hedderson 2004;

62   Thiede 2004; Klak, Hanáček & Bruyns 2017b; for authors and species numbers see Table 1).

63   Species of Mesembryanthemoideae and Ruschioideae, commonly referred to as 'mesembs'

64   (Mesembryanthema; Hartmann 1991), were found in molecular phylogenetic studies to be

65   reciprocally monophyletic (e.g., Klak et al. 2003; Thiede 2004; Klak, Hanáček & Bruyns 2017b).

66   Mesembryanthemoideae and Ruschioideae, as well as their sister-group relationship, are

67   supported by morphological characters. Mesembryanthemoideae + Ruschioideae can be

68   distinguished from the remaining Aizoaceae by raphid bundles of calcium oxalate (in contrast to

69   calcium oxalate druses), the presence of petals of staminodial origin, half-inferior or inferior

70   ovary and a base chromosome number of $x = 9$ (Bittrich & Struck 1989). The conspicuous

71   loculicidal hygrochastic fruit capsules of ca. 98% of the species (Ihlenfeldt 1971; Parolin 2001;

72   Parolin 2006) are lacking in Acrosanthoideae, for which xerochastic, parchment-like capsules are

73   apomorphic, but are also predominant in subfamily Aizooideae (Bittrich 1990; Klak, Hanáček &

74   Bruyns 2017a). In Aizooideae, however, valve wings of the capsules are either absent or very

75   narrow, while they are well developed in Mesembryanthemoideae + Ruschioideae (Bittrich &

76   Struck 1989).

77   The capsules of Mesembryanthemoideae and Ruschioideae differ in the structure of their

78   expanding keels. The expanding keels are of purely septal origin in Mesembryanthemoideae, and

79   mainly of valvar origin in Ruschioideae (Hartmann 1991). In floral structure, Ruschioideae are

80   characterized almost always by crest-shaped (lophomorphic) nectaries and a parietal placentation

81   (Hartmann & Niesler 2009), while Mesembryanthemoideae possess plain shell-shaped

82   (coilomorphic) nectaries and a central placentation.

83   **Subfamilies of Aizoaceae: origin and distribution of major clades**

84   Subfamily Sesuvioideae, sister to the rest of Aizoaceae, originated in Africa/Arabia suggesting

85   an African origin for the entire family (Bohley et al. 2015). While Sesuvioideae and Aizooideae

86   dispersed as far as Australia and the Americas (Bohley et al. 2015; Klak, Hanáček & Bruyns

87   2017b), Acrosanthoideae, Mesembryanthemoideae and Ruschioideae are most diverse in

88   southern Africa. Only a small number of Ruschioideae species are found outside of this area.

89   *Delosperma* N.E.Br. is native to Madagascar and Réunion and expands with less than ten species

90   along the East African mountains into the south-eastern part of the Arabian Peninsula (Hartmann

91   2016, Liede-Schumann & Newton 2018). Additionally, in Ruschioideae there are nine halophytic

92   species endemic to Australia (Prescott & Venning 1984; Hartmann 2017a; Hartmann 2017b),

93   and possibly one species to Chile (Hartmann 2017a).

94   In southern Africa, most species of Acrosanthoideae, Mesembryanthemoideae and Ruschioideae

95   are native to the Winter Rainfall Region (Verboom et al. 2009; Valente et al. 2014) in the GCFR.

96   Acrosanthoideae with only six species is endemic to mesic fynbos, whereas

97   Mesembryanthemoideae and Ruschioideae are speciose in more arid Succulent Karoo vegetation

98   (Klak, Hanáček & Bruyns 2017a).

99   **Within Ruschioideae: relationships of major clades**

100   Ruschioideae constitute the largest clade of Aizoaceae with estimated species richness of ca.

101   1600 (Stevens 2001, onwards; Klak, Bruyns & Hanáček 2013). Within Ruschioideae three tribes,

102   Apatesieae**,** Dorotheantheae, and Ruschieae s.l., have been distinguished based on unique

103   combinations of nectary and capsule characters (Chesselet, Smith & Van Wyk 2002). These

104   three tribes form well supported clades in phylogenetic analyses (Klak et al. 2003; Thiede 2004;

105   Valente et al. 2014). Ruschieae s.l. are further characterized by the possession of wideband

106   tracheids (Landrum 2001), endoscopic peripheral vascular bundles in the leaves (Melo-de-Pinna

107   et al. 2014), smooth and crested mero- and holonectaries, well-developed valvar expanding

108   tissue in the capsules (Hartmann & Niesler 2009), the loss of the *rpoC1* intron in the chloroplast

109   DNA (cpDNA; Thiede, Schmidt & Rudolph 2007) and the possession of two *ARP* (Asymmetric

110   Leaves1/Rough Sheath 2/Phantastica) orthologues in the nuclear DNA (Illing et al. 2009); the

111   duplication most likely took place after the divergence of the Ruschioideae from the

112   Mesembryanthemoideae, with the subsequent loss of one paralogue in Apatesieae and

113   Dorotheantheae (Illing et al. 2009).

114   Within Ruschieae s.l. ('core ruschioids' *sensu* Klak, Reeves & Hedderson 2004), Klak et al.

115   (2003) additionally revealed two clades with strong support, Ruschieae s.str. and a clade

116   consisting only of members of *Drosanthemum* Schwantes. Species of *Delosperma*, considered

117   closely related to *Drosanthemum* due to a papillate epidermis, often broad, flat mesophytic

118   leaves, relatively simple hygrochastic fruits and a meronectarium have been described with

119   *Drosanthemum* in tribe Delospermeae Chesselet, G.F. Smith & A.E. van Wyk (2002). In

120   phylogenetic studies, however, *Delosperma* species are nested in Ruschieae s.str. (except for a

121   few species, e.g., *Drosanthemum asperulum* and *D. longipes*, which have been assigned in turn

122   to either *Delosperma* or *Drosanthemum*). Consequently, Chesselet, Van Wyk & Smith (2004)

123   included *Delosperma* in Ruschieae s.str. and coined the monogeneric Drosanthemeae Chesselet,

124   G.F. Smith & A.E. van Wyk as a distinct tribe sister to Ruschieae s.str. (in the following

125   Drosanthemeae + Ruschieae = core ruschioids; Table 1).

126   While Ruschieae are characterized by fused leaf bases (Chesselet, Van Wyk & Smith 2004), an

127   apomorphic trait is less obvious for its sister tribe Drosanthemeae. Hartmann & Bruckmann

128   (2000) suggested capsules with a bipartite pedicel, of which the lower part appears darker due to

129   an inner corky layer, and the upper part often thinner and agreeing in surface and colour with the

130   capsule base. More generally, species of Drosanthemeae are considered mesomorphic, compared

131   to the highly succulent, xeromorphic Ruschieae (Klak, Bruyns & Hanáček 2013).

132   **Core ruschioids: relationships of lineages**

133   A sister-group relationship of Drosanthemeae and Ruschieae has been revealed by molecular

134   phylogenetic analyses (Klak, Bruyns & Hanáček 2013). Whether both groups are reciprocally

135   monophyletic (and in which circumscription) is less clear (e.g., Klak, Hanáček & Bruyns 2017b).

136   For example, molecular phylogenies identified two species erroneously included in

137   Drosanthemeae. One of these, *Drosanthemum diversifolium* L.Bolus, was first transferred to

138   *Knersia* H.E.K.Hartmann & Liede, a monotypic genus placed in Ruschieae (Hartmann & Liede-

139   Schumann 2013), and later to *Drosanthemopsis* Rauschert (Ruschieae) by Klak, Hanáček &

140   Bruyns (2018). The second species, *Drosanthemum pulverulentum* (Haw.) Schwantes, with a

141   xeromorphic epidermis untypical for Drosanthemeae, was retrieved as member of the highly

142   succulent clade "L1" in Ruschieae (Klak, Bruyns & Hanáček 2013; not yet formally transferred).

143   With these corrections, Drosanthemeae comprise a single genus, *Drosanthemum*, with 114

144   species presently recognized and a wide distribution in the GCFR with the centre of diversity in

145   the Cape Floristic Region (Hartmann 2017a, Van Jaarsveld 2015, 2018, Liede-Schumann, Meve

146   & Grimm 2019).

147   ***Drosanthemum* (Drosanthemeae) systematics**

148   Within *Drosanthemum*, five floral types have been distinguished, differing mainly in number,

149   position and relative length of petaloid staminodes (Rust, Bruckmann & Hartmann 2002; Fig. 1).

150   Also, ten types of capsules have been described, differing in size and shape of the capsule base

151   and the capsule membrane, and the presence or absence of a closing body (Hartmann &

152   Bruckmann 2000). Based on a combination of these flower and fruit types, Hartmann (2007)

153   proposed a subdivision of *Drosanthemum* in eight subgenera. Later, Hartmann & Liede-

154   Schumann (2014) proposed two more subgenera based on additional vegetative morphology, and

155   also suggested the union of two of the previously described subgenera. This reflects an unusually

156   broad variation in flower and capsule types encountered in the genus compared with other

157   Aizoaceae genera.

158   Despite this extraordinary morphological diversity, molecular phylogenetic studies of

159   *Drosanthemum* have hitherto been restricted to few species: nine species studied for ten cpDNA

160   regions in Klak, Bruyns & Hanáček (2013) and 16 species studied for two cpDNA regions and

161   the nuclear-encoded internal transcribed spacer (ITS) region of the 35S ribosomal DNA cistron

162   in Hartmann & Liede-Schumann (2013). Obtaining increased species coverage representative for

163   the phenotypic and taxonomic diversity present in *Drosanthemum* is challenging partly due to

164   ambiguous species assignment to either *Drosanthemum* or *Delosperma* (Hartmann & Liede-

165 Schumann 2014), but mainly due to challenges in attributing specimens to published species
166 names in *Drosanthemum*. Ambiguous and/or overlapping diagnostic characters are common
167 among closely related species and also present between subgenera or genera. Specimens of
168 species flocks and cryptic species (Liede-Schumann, Meve & Grimm 2019) are often hard to
169 identify with certainty, a fact that might have hampered investigation of the genetic
170 differentiation among *Drosanthemum* species. In this study, we build on Heidrun Hartmann's
171 huge field collections of identified specimens of *Drosanthemum*. The present study would not
172 have been possible without her enduring commitment to collect, diagnose, and formally name
173 species in the Aizoaceae.

174 We present a phylogenetic study of *Drosanthemum* covering more than 64% of the species
175 richness (73 of 114 recognized species) representing all subgenera. We analyse chloroplast and
176 nuclear DNA sequence variation using phylogenetic tree and network approaches and assemble a
177 taxonomically-verified occurrence dataset. Specifically, we test whether: 1) *Drosanthemum* is a
178 monophyletic lineage sister to Ruschieae; 2) the morphologically delineated subgenera are
179 monophyletic, in particular, whether the most species-rich subgenus *Drosanthemum* is
180 monophyletic or, alternatively, a "dustbin" for species that cannot be assigned to other subgenera
181 based on morphology; 3) all accessions within currently recognized species are indeed each
182 other's closest relative; and 4) the clades detected in this study have distinct geographic
183 distributions in the GCFR.

Material and Methods

Taxon sampling

186 We established a collection of georeferenced and identified *Drosanthemum* samples; each
187 sample was only included if sufficient material was available to identify key characteristics. The
188 full collection ('core collection'; n = 997 samples) represents the most comprehensive sampling
189 of the currently recognized *Drosanthemum* species, covering 85 species in total, with each
190 species represented by up to 30 georeferenced samples (range: 1–30; mean: 5 samples per
191 species). This core collection consists of 590 samples identified to subgenus, plus 407 identified
192 to species. The subgeneric classification follows Hartmann (2007) and Hartmann & Liede-
193 Schumann (2014).

194   A subset of the core collection was used to generate the molecular dataset; this subset comprised

195   134 accessions of *Drosanthemum*, covering 73 of the recognized species, with the more

196   widespread and morphologically variable species represented by up to 5 accessions. To cover the

197   full distribution in the larger subgenera, the molecular dataset comprises 21 accessions identified

198   to subgenus, several of which most likely represent hitherto undescribed species: subg.

199   *Drosanthemum* (10 accessions), subg. *Vespertina* (8 accessions), subg. *Xamera* (2 accessions),

200   and subg. *Ossicula* (1 accession). Geographic distributions of the subgenera that were

201   corroborated with phylogenetic inference in this study (i.e., inferred clades, see *Results*) were

202   plotted on a map using the elevation above sea level data from the WorldClim climate layers

203   (Hijmans et al. 2005), with a spatial resolution of 30' using the RASTER library v2.8-19 (Hijmans

204   2019) in R v3.5.3 (R Core Team, 2019). Geographic references for the core collection are

205   available at the Dryad digital repository (Liede-Schumann et al. 2019).

206   For outgroup comparison we selected a broad spectrum of species representing the three

207   remaining tribes of Ruschioideae: Apatesieae (two accessions representing one species),

208   Dorotheantheae (three species), and Ruschieae (49 accessions representing 47 species and 42

209   genera). We used the cpDNA dataset of Klak, Bruyns & Hanáček (2013) pruned to include one

210   to several accessions of each Ruschieae clade (depending on clade size) with an additional nine

211   species sequenced in previous studies of the present authors. Nuclear ITS sequences were

212   downloaded from GenBank for accessions identical to the cpDNA dataset; in five cases different

213   accessions of the same species had to be used: *Dorotheanthus bellidiformis* (Burm.f.) N.E.Br.,

214   *Cheiridopsis excavata* L.Bolus, *Corpuscularia lehmannii* (Eckl. & Zeyh.) Schwantes,

215   *Jacobsenia kolbei* (L.Bolus) L.Bolus & Schwantes, and *Prepodesma orpenii* (N.E.Br.) N.E.Br. A

216   species shown by Klak, Bruyns & Hanáček (2013), to belong in Ruschieae clade L1,

217   *Drosanthemum pulverulentum* (Haw.) Schwantes, was regarded as part of the outgroup.

218   **PCR and sequencing**

219   We targeted four cpDNA markers and the nuclear rDNA ITS region. These included two cpDNA

220   markers, the *trn*S-*trn*G intergenic spacer region and the *rpl*16 intron, that were found to have the

221   highest intra-generic divergence amongst the seven *Drosanthemum* accessions used by Klak,

222   Bruyns & Hanáček (2013); these regions were amplified using the primers and protocols

223   provided in the original paper. In addition, two cpDNA intergenic spacers, *trnQ–5'rps16* and

224 3'*rp*S*16*–5' *trn*K, were amplified with primers trnQ[(UUG)] and rpS16x1 and with primers

225 rpS16x2F2 and trnK[(UUU)], respectively (Shaw et al. 2007). The nuclear ITS region was amplified

226 as detailed in Hassan, Thiede & Liede-Schumann (2005).

227 Total genomic DNA was extracted from seedlings or from herbarium specimens using the

228 DNeasy Plant MiniKit (Qiagen, Hilden, Germany), following the protocol of the manufacturer.

229 For sequencing, the PCR products were sent to Entelechon (Regensburg, Germany) or Eurofins

230 (Ebersberg, Germany) resulting in 473 new sequences of *Drosanthemum* species produced in

231 this study. Forward and reverse sequences were aligned with CODONCODE ALIGNER, v.3.0.3

232 (CodonCode Corp., Dedham, Massachusetts, U.S.A.). Sequence data of individual marker

233 regions were aligned with OPAL (Wheeler & Kececioglu 2007) and checked visually using

234 MESQUITE v.3.51 (Maddison & Maddison 2018). All sequences newly generated in this study

235 have been submitted to ENA (for accession numbers see supplemental information S1).

Phylogenetic analyses

237 **Phylogenetic tree inference**: We used maximum likelihood (ML) and non-parametric

238 bootstrapping (BS) analysis on a concatenated cpDNA dataset (comprising all four regions)

239 including only *Drosanthemum* species ('*Drosanthemum'* dataset: 134 accessions), and on a

240 dataset also including outgroup species ('Ruschioideae' dataset: 188 accessions; see *Taxon*

241 *sampling*) to infer the placement of the *Drosanthemum* species in relation to the other

242 Ruschioideae lineages. Note that prior to this concatenated cpDNA analysis, each marker was

243 analysed individually and in various division schemes (several data matrices were tested:

244 partitioned and unpartitioned, also including or excluding the most-divergent and length-

245 polymorphic *rps*16-*trn*Q spacer region, and including/excluding an ITS partition; raw data, code

246 and results are available at Dryad, Liede-Schumann et al. 2019). No supported topological

247 discordances were present; thus we used a concatenated four-markers cpDNA dataset. ML tree

248 inference and BS analysis relied on RAxML v. 8.0.20 (Stamatakis 2014), partitioned and set to

249 allow for site-specific variation modelled using the 'per-site rate' model approximation of the

250 Gamma distribution (Stamatakis 2006). Duplicated sequences were reduced to a single sequence

251 resulting in 131 accessions in the ML cpDNA tree of *Drosanthemum*. The same RAxML settings

252 were used for the 'Ruschioideae' dataset. To obtain probability estimates for the most likely

253 *Drosanthemum* (ingroup) root, we used the evolutionary placement algorithm (EPA; Berger,

254 Krompass & Stamatakis 2011) implemented in RAxML and following the analytical set-up of

255 Hubert et al. (2014) and Grímsson et al. (2018). EPA provides probability estimates (Berger,

256 Krompass & Stamatakis 2011) for placing a query sequence (here: outgroup taxa representing

257 the Ruschieae) within a given topology (here: ML *Drosanthemum* cpDNA tree) offering

258 identifying a consensus outgroup-based root while minimising potential biases (e.g. long-branch

259 attraction, LBA; Bergsten 2005). To do so, we queried a set of 47 Ruschieae species and

260 calculated a probability estimate (p_R) by averaging the likelihood weight ratios of query taxa per

261 inferred rooting scenario over all queried taxa.

262 **Phylogenetic network inference**: We investigated competing support patterns within

263 *Drosanthemum* by means of BS consensus networks (Holland & Moulton 2003; Grimm et al.

264 2006; Schliep et al. 2017) using with SplitsTree v. 4.1.13 (Huson & Bryant 2006) and 1000

265 bootstrap (pseudo-) replicate RAxML trees (see paragraph above). The number of necessary BS

266 replicates was determined using the extended majority bootstrap criterion (Pattengale et al.

267 2009). Additionally, we investigated within-lineage differentiation of subclades within

268 *Drosanthemum* ('subclade' refers here to the nine clades within the genus *Drosanthemum*

269 defined in the Results section) using median-joining (MJ; Bandelt, Forster & Röhl 1999)

270 networks for the cpDNA dataset and statistical parsimony (SP; Templeton et al. 1992) networks

271 for the ITS data. MJ networks were computed with NETWORK v.5.0.0.3 (Fluxus; available online

272 www.fluxus-engineering.com/ sharenet.htm) with default settings and no character weighting

273 and SP networks with PEGAS v0.11 (Paradis 2010) in R. In the MJ network analyses, we used

274 reduced sequence alignments differentiating four sequence patterns at the intra-subclade level: (*i*)

275 single-nucleotide polymorhisms (SNPs); (*ii*) insertions, duplications and deletions (indels),

276 represented by a single character because gaps are treated as 5th base by NETWORK by default;

277 (*iii*) length-polymorphic sequence motifs (LP, such as multi-A motifs, which were only

278 considered when including mutations additional to length variation; this category also includes

279 more complex length-polymorphic patterns such as length-polymorphic AT-dominated sequence

280 regions); and (*iv*) oligo-nucleotide motifs (ONM, short motifs with apparently linked mutations

281 that can slightly differ in length, which were treated as a single mutational event; inversions, like

282 the ones found in the pseudo-hairpin structure of the *trnK-rps16* spacer, are a special form of

283 ONMs). The highly divergent, length-polymorphic 'high-div' region characterising the 5' end of

284   the *rps*16-*trn*Q intergenic spacer, was generally excluded from the analysis but included in the

285   haplotype documentation (see Liede-Schumann et al. 2019: file Haplotyping.xlsx).

286   The reasoning for the use of MJ and SP networks is because there were few consistent mutations

287   at the intrageneric level within subclades — this results in a flat likelihood surface of the tree

288   space and, in this situation, parsimony can be more informative than probabilistic approaches

289   (Felsenstein 2004). In contrast to phylogenetic trees, MJ networks include all equally

290   parsimonious solutions to a dataset and produce *n*-dimensional splits graphs that can include

291   topological alternatives. Also, MJ and SP haplotype networks directly depict ancestor-

292   descendant relationships, and hence, can assist in deciding whether inferred clades in the tree are

293   monophyletic in a strict sense, i.e. groups of inclusive common origin (Hennig 1950; see also

294   Felsenstein 2004, chapter 10). Because the MJ networks can easily become diffuse or complex,

295   especially when analysing interspecific relations, we summarized the inferred haplotypes into

296   haplotype groups for visualizing and interpreting MJ networks.

297   Results

298   Patterns of DNA sequence diversity

299   We targeted the most variable cpDNA gene regions currently known for Aizoaceae, which

300   provided a relatively high number of distinct alignment patterns (Table 2), although each cpDNA

301   marker on its own provides low topological resolution (single plastid gene-region ML trees and

302   BS consensus networks are provided in Liede-Schumann et al. 2019). Length-polymorphism was

303   common, hence, the high proportion of gaps (undetermined cells) in the alignments, but often

304   restricted to duplications or deletions, rarely insertions, and explicitly alignable. An exception

305   was the *rps*16-*trn*Q intergenic spacer, which includes regions with extreme length-polymorphism

306   and highly complex sequence patterns that are only alignable amongst closely related species. A

307   notable feature is a 'pseudo-hairpin' sequence found in the *trn*K-*rps*16 intergenic spacer, which

308   includes a partly clade-diagnostic strictly complementary upstream-downstream sequence pattern

309   composed of duplications of two short sequence motifs and subsequent deletions and a

310   "terminal" inversion (shown in the coding example in supplemental information S2, Fig. S2-A;

311   for more details see Liede-Schumann et al. 2019: Haplotype.xlsx).

312   In general, cpDNA sequence patterns in *Drosanthemum* are highly diagnostic at and below the

313   level of major clades, in most cases allowing identification of haplotypes or clade-unique

314   substitution pattern. This includes a few, potentially synapomorphic (*sensu* Hennig 1950:

315   uniquely shared derived traits) single-base mutations in generally length-homogenous sequence

316   portions (see Liede-Schumann et al. 2019). Indel patterns appear to be largely homoplastic, but

317   sometimes diagnostic at the species level or for species flocks. In contrast, mutation patterns in

318   the length-homogeneous (SNPs) and length-polymorphic regions (LP, indels, ONMs) are largely

319   congruent, with few conflicting signals, for taxon splits.

320   The nuclear-encoded ITS region has low divergence and contains little signal for tree

321   discrimination, which is typical for the Aizoaceae (e.g., Klak, Bruyns & Hanáček 2013), and was

322   not included for defining major clades or testing their coherence with the earlier proposed

323   subgenera. Still, the genetic diversity present (Table 2) allows for the identification of more

324   ancestral vs. more derived genotypes (supplemental information S3), which were mapped onto

325   the cpDNA tree (Fig. 2).

326   **Phylogenetic inference and potential *Drosanthemum* roots**

327   The ML tree of *Drosanthemum* (based on the concatenated cpDNA dataset) indicates nine

328   moderately (>65% BS support) to well supported (>75% BS support) clades (Fig. 2). Seven of

329   these group in two major clades, with high support for the clade I+II+III+IV (98% BS support;

330   addressed informally as '*Drosanthemum* core clade', Fig. 3) and low support for the second

331   clade V+VI+VII (58% BS support). Clades VIII and IX have ambiguous affinities (results not

332   shown; for full documentation see Liede-Schumann et al. 2019). Two species, *D. longipes* (sister

333   to clade VII) and *D. zygophylloides* (sister to VIII) are not included in the nine described clades

334   (see *Discussion – Phylogenetic inference reflects taxonomic classification*). Notably, the nine

335   clades overall group into six lineages (clades I–IV, V+VI, VII+*D. longipes*, VIII, XI, and

336   *D. zygophylloides*), but relationships among the six lineages were weakly supported.

337   Specifically, the earliest branching events in the ML tree are ambiguously resolved (Fig. 2)

338   The ML tree of Ruschioideae (based on the 'Ruschioideae' dataset) inferred *Drosanthemum* a

339   monophyletic sister to Ruschieae (100% BS support, Fig. S4.1), supporting the 'core ruschioids"

340   hypothesis (Table 1; for details see Liede-Schumann et al. 2019). In this tree, the topology within

341   *Drosanthemum*, however, differs in parts (clade VIII and IX successive sister to the rest; not

342   supported) from the tree inferred by the analysis of the '*Drosanthemum*' dataset (Fig. 2; both

343   datasets comprise the same four concatenated cpDNA regions). Taken together, phylogenetic

344   inference is consistent with a rapid initial diversification within *Drosanthemum* that was

345   potentially too fast to leave a signal in cpDNA sequence variation in the studied markers.

346   Placement of the 49 queried outgroup taxa indicates eleven potential *Drosanthemum* root

347   positions (Fig. 3). However, six of these positions are unlikely considering the probability

348   estimates p_R (an order of magnitude lower), number of supporting queries (0 to 2), and

349   phylogenetic evidence (supplemental information S4: Table S4). The remaining five root

350   positions are summarized as follows: scenario 1, clade I–IV sister to clade V–IX, supported by

351   33 queries and $p_R = 0.26$ (Fig. 2; supplemental information S4: Fig. S4.2); scenario 2, clade IX

352   sister to the rest, eight queries and $p_R = 0.23$ (supplemental information S4: Fig. S4.3); scenario

353   3, clade VIII + *D. zygophylloides* sister to the rest, one query and $p_R = 0.14$ (supplemental

354   information S4: Fig. S4.4); scenario 4, cladeV–VII + *D. longipes* sister to clade I–IV + VIII + *D.*

355   *zygophylloides* + IX, four queries and $p_R = 0.14$ (supplemental information S4: Fig. S4.5);

356   scenario 5, clade I–IV + VIII + *D. zygophylloides* sister to clade V–IIV + *D. longipes* + IX,

357   supported by zero queries and $p_R = 0.14$ (supplemental information S4: Fig. S4.6). Because the

358   outgroup samples are notably distant in the targeted plastid gene regions to *Drosanthemum*

359   favouring attraction of most distinct accessions, scenarios 3–5 may be artefacts generated by

360   outgroup-ingroup (long) branch attraction. Scenario 1 is identified as the most likely root

361   position and has additionally the highest probability estimate and number of supporting queries

362   by the distribution of ITS genotypes, indicating underived variants in clade I and V and both un-

363   and derived ITS variants in the smaller clades outside '*Drosanthemum* core clade' (Fig. 2; see

364   also *Results, Identification of ITS genotypes*). Overall, the results obtained by outgroup-EPA are

365   consistent with a fast radiation generating the main lineages early in the evolution of

366   *Drosanthemum*.

367   **Inter- and intra-clade differentiation patterns**

368   The haplotype analyses (of each gene region) is in overall congruence with the combined

369   cpDNA tree (Fig. 2). However, in some genes and/or clades coherent mutational patterns are

370   shared by several species, which lack uniquely shared sequence patterns in other gene regions.

371   Thus, detailed haplotype networks (Figs 4–7) further illuminate phylogenetic relationships in

372   clades VII–IX (and the two isolated species *D. longipes* and *D. zygophylloides*), and further

373   corroborate subgroups within clades I, III, and V (Figs. 2, 3).

374   Clade I is divided into three subclades and the haplotype analysis supports a monophyly of

375   clades Ia and Ic, but not Ib (Fig. 4A–D). Members of clade Ib are characterized by haplotypes

376   either ancestral to those found in clades Ia and Ic (*rpl16* intron, *trnK-rps16*) or unique and

377   strongly divergent from each other (*rps*16-*trn*Q). Clade II haplotypes are more similar to

378   ancestral haplotypes in clade I than to those in clades III or IV. The haplotypes in clades III and

379   IV are very similar to each other (Fig. 4E–H). Clade III is divided into a more diverse (likely

380   paraphyletic) grade IIIa and a monophyletic clade IIIb (Figs 2, 3, 4E–H). Within clade III, clade

381   IIIb forms an increasingly derived (monophyletic) lineage (*D. luederitzii* + *D. obibense* → *D.*

382   *nollothense* → *D. brevifolium* + *D. ramossissimum*) that starts with grade IIIa individuals having

383   *D. cymiferum*-like morphology but are genetically distinct from *D. cymiferum*. Clade V includes

384   two sequentially coherent and mutually exclusive (reciprocally monophyletic) clades, Va and Vb

385   (Fig. 3). In general, haplotypes of clade Vb show more unique shared mutational patterns than

386   those of clade Va (Fig. 5A–D). Figure 5A–D also includes the relatively similar haplotypes of

387   the sister lineage, clade VI, which can be used to root the MJ networks (note that the edge length

388   reflects the difference in the variable genetic patterns within clade V and does not include

389   sequence patterns uniquely found in clade VI). Two markers, *trn*K-*rps*16 and *trn*S-*trn*G, reflect

390   the potential reciprocal monophyly of both clades. *Drosanthemum gracillimum* is not included in

391   clade Va or Vb (Figs 2, 3). Only two of the considered cpDNA markers are available for this

392   species, *trn*S-*trn*G and *rps*16-*trn*Q, with no lineage-diagnostic sequence pattern and obviously

393   showing the putative ancestral haplotype within clade V (Fig. 5A–D).

394   Whereas haplotypes can be very divergent at the inter- and even intra-clade level (e.g. Fig. 4),

395   they are relatively similar to each other in the smaller clades VII–IX (Fig. 5E–H).

396   *Drosanthemum longipes trn*S-*trn*G and *rps*16-*trn*Q haplotypes are highly similar to those of

397   clade VII. Each gene region has a series of mutational patterns in which *D. longipes* and all

398   members of clade VII are distinct from clade VIII and IX. In the lowest-divergent *trn*K-*rps*16

399   intergenic spacer region, the *D. longipes* haplotype can directly be derived from the one of clades

400   VIII and IX (Fig. 5E–H). *Drosanthemum longipes* is genetically closer to the putative

401 *Drosanthemum* ancestor than to members of clade VII. In contrast, the haplotypes of *D.*
402 *zygophylloides* are visibly unique within the genus (Fig. 5E–H), which is also reflected in its
403 long terminal branches in the cpDNA tree (Fig. 2).

Identification of ITS genotypes in *Drosanthemum*

405 Analysis of nuclear ITS sequence variation reveals 62 genotypes, for which SP analysis produces
406 an overall, but highly reticulated, star-shaped network with genotypes linked to various cpDNA
407 lineages in the centre (Fig. 6; supplemental information S3). The least derived but most common
408 genotypes are found in distantly related clades: genotype 33 in clade I and genotype 6 clade V
409 (Fig. 6). Genotypes 6 and 33 resemble the consensus of all ITS genotypes differing only by a
410 single point mutation (note that genotype 33 collects several subtypes differing in an indel
411 pattern that is ignored by the SP network; supplemental information S3; for details see Liede-
412 Schumann et al. 2019: files Haplotype.xlsx, DataSummary.xlsx). Genotype 3 is shared by
413 members of clade VII and IX and is central to most other (including the most common 33 and 6;
414 Fig. 6). Clades VII–IX and the two phylogenetically isolated species, *D. longipes, D.*
415 *zygophylloides*, have unique, derived genotypes. The ITS genotypes of clades II, IIIb and IV can
416 be derived from the most ancestral ones in clade I and IIIa. The fact that ITS evolution, a
417 stepwise derivation of a putatively ancestral, consensus sequence into genotypes that are unique
418 within clades and can be mapped on the cpDNA phylogeny (Fig. 2) indicates that ITS
419 differentiation in the '*Drosanthemum* core clade' is in overall congruence with the cpDNA tree.

Geographical clade structure in *Drosanthemum*

421 All clades retrieved in the present analysis show their own characteristic distribution pattern. All
422 clades are present in the south-western Cape, and three clades (VI, VII, VIII) hardly extend
423 beyond this narrow region. The species-rich clades I, II, and IV cover the largest areas. Clade V
424 extends along the southern Cape coast and clades III and IX extend along the West coast. (Fig.
425 7).

426

427 **Discussion**

428 **Genetic differentiation patterns indicate fast radiation initiating**

429 **diversification within *Drosanthemum***

430 Phylogenetic analysis, in-depth haplotype analyses of cpDNA, and mapping of ITS evolution on

431 the ML cpDNA tree point towards a rapid initial diversification within the genus *Drosanthemum*.

432 The best outgroup-EPA inferred rooting position indicates *Drosanthemum* species to group in

433 two large clades, with clade I–IV, the '*Drosanthemum* core clade', sister to clade V–IX (Fig. 2).

434 The uncertainty in root position (Fig. 3; supplemental information S4) is consistent with a pattern

435 expected in initial radiations (Graham & Iles 2009; Saarela et al. 2007). The star-like (but

436 reticulated) structure of the SP network (nuclear ITS data) suggests an initial bottleneck early in

437 the evolution of *Drosanthemum* followed by rapid diversification (Fig. 6, supplemental

438 information S3). Similarly, the plastid sequence variation provides sufficient information to

439 resolve nine well-supported clades within the genus *Drosanthemum*. However, the 'backbone'

440 relationships among the nine clades, or more specifically, the six lineages, are not resolved (Figs.

441 2, 3). Taken together, the difficulties to separate and clarify the exact sequence of early

442 branching events is a characteristic pattern in rapid evolutionary radiations among the plant tree

443 of life, and has been found at various phylogenetic levels, for example, in Saxifragales (Fishbein

444 et al. 2001), within the genus *Hypericum* (Hypericaceae; Nürk et al. 2013; 2015) and in a group

445 of South American *Lithospermum* (Boraginaceae; Weigend et al. 2010). It remains to be seen,

446 however, whether analyses of nuclear markers apart from ITS support the patterns retrieved here.

447 **Phylogenetic inference reflects taxonomic classification**

448 Within *Drosanthemum,* nine clades are revealed, which generally correspond to the recognized

449 subgenera (Hartmann 2017a), although some exceptions exist. The deviations in morphology-

450 based classification and phylogenetic evidence produced in this study reveals cryptic species and

451 several new relationships. For example, the species *D. zygophylloides*, *D. gracillimum*, and

452 *D. longipes*, have either never been included into the subgeneric classification

453 (*D. zygophylloides*), or phylogenetic evidence indicates affinities different from classification

454 (*D. gracillimum, D. longipes*; Fig. 2). Considering our results, these species cannot be included

455   in any of the proposed subgenera (Hartmann 2017a). Note that both *D. longipes* and the species

456   in clade IX shed leaves in summer and resprout with the winter rains.

457   Subgenus *Drosanthemum* is revealed as biphyletic, with most of its species in clade I, sister to

458   clade II (subgenus *Xamera*; see below). *Drosanthemum hispidum*, the type species of

459   *Drosanthemum*, groups in clade I (subclade Ic; Fig. 2). The rest of the species classified in

460   subgenus *Drosanthemum* group within clade III. No morphological diagnostic characters are

461   obvious to distinguish the clade III species from those in clade I, and thus, clade III is not yet

462   circumscribed as a tenth subgenus. Likewise, subgenus *Drosanthemum* species in clade I group

463   in three subclades Ia, Ib, and Ic, but morphological characters defining these clades cannot yet be

464   named. Hence, this species-rich subgenus is obviously biphyletic, but species assigned to it are

465   not distributed all over the tree, i.e. subgenus *Drosanthemum* does not appear to be a "dustbin"

466   for species that cannot be assigned based on morphology to any other subgenera.

467   The discussed clades I–III, together with clade IV, constitute the informally named

468   '*Drosanthemum* core clade'. Clade IV corresponds to the night-flowering subgenus *Vespertina*

469   that is characterized by flowers of the long cone type (Rust, Bruckmann & Hartmann 2002).

470   Subgenus *Xamera* (clade II) is characterized by usually six-locular capsules and four tiny

471   spinules below the capsule stalk and on older lateral branches (Hartmann 2007). *Drosanthemum*

472   *delicatulum* and *D. subclausum* of clade II also show this character, so that their listing under

473   subgenus *Drosanthemum* in Hartmann (2017a: 508, 532) is clearly erroneous (as is also indicated

474   by the listing of *D. subclausum* among the species of *Xamera* in Hartmann (2017a: p 495).

475   Conversely, *D. dejagerae* L.Bolus, attributed to *Xamera* by Hartmann (2007, 2017a) due to the

476   presence of a six-locular capsules characteristic for the subgenus, is placed in clade Ic (subgenus

477   *Drosanthemum* p.p.).

478   Of the six remaining subgenera, four — *Speciosa* (clade Va), *Ossicula* (clade Vb), *Necopina*

479   (clade VI), and *Quastea* (clade VII) — group in one clade that is, however, not well supported

480   (Fig. 2) and also lacks obvious commonly shared, derived morphological characters. In

481   particular, the stout and often large capsules (to 1 cm diam.) of subgenus *Speciosa* (Hartmann &

482   Bruckmann 2000) contrast strongly with the tender and smaller capsules of the other three

483   subgenera. However, bone-shaped closing bodies in the capsules, considered unique for

484   subgenus *Ossicula*, have also been found in capsules of *Speciosa* species (Hartmann & Le Roux

485 2011), reducing their potential as a diagnostic character for *Ossicula*. This is illustrated by *D.*

486 *austricola* L.Bolus, which is retrieved in subclade Va, corresponding to subgenus *Speciosa*,

487 despite its conspicuous bone-shaped closing body, a character for which it was placed in

488 *Ossicula* by Hartmann (2008).

489 While the subgeneric classification of *Drosanthemum* (Hartmann 2007; Hartmann & Liede-

490 Schumann 2014) is largely confirmed, a few unexpected placements of single species deserve

491 mentioning. Of the three samples of *Drosanthemum cymiferum*, attributed to subgenus *Quastea*

492 in Hartmann (2007), only one sample was retrieved in the *Quastea* clade VII, the other two in

493 clade III (*Drosanthemum* p.p.). This species was studied in some more detail in Liede-

494 Schumann, Meve & Grimm (2019), who did not find any consistent morphological differences

495 between these samples and suggested a case of cryptic speciation (following the definition of

496 Bickford et al. 2007). A similar case is found in *D. muirii* L.Bolus, of which the two samples are

497 retrieved with good support in subclades Ia and Ic, respectively (Fig. 2).

Distinct geographic distributions in the Greater Cape Floristic Region

499 Inside the genus *Drosanthemum*, six lineages originate from a soft polytomy (precisely, they root

500 in an unsupported part of the tree; Fig. 2), suggesting a radiation right at the start of the

501 evolutionary history of *Drosanthemum*. To which extent this radiation was driven by ecological

502 or geographical factors remains an open question. Interestingly, several clades comprising only

503 3–6 species are distributed over a restricted geographical range: clade VI *Necopina* (6 spp), clade

504 VII *Quastea* (4 spp), and clade VIII *Quadrata* (3 spp) are restricted to the western part of the

505 Cape Mountains (Fig. 7, F–I). One species-poor lineage, clade IX *Decidua* (3 spp.), extends

506 along the West Coast into Namibia Fig. 7, J). Species in clade V, 14 in clade Va *Speciosa* and 6

507 in clade Vb *Ossicula* are almost restricted to the fynbos of GCFR (Fig. 7, F), whereas the

508 comparatively higher species number in *Speciosa* might be the result of more thorough studies in

509 this showy, horticulturally valuable subgenus (e.g., Hartmann 2008, Hartmann & Le Roux 2011).

510 Notably, these clades are genetically and morphologically coherent, that is, possess unique and

511 derived sequence patterns as well as characteristic morphologies.

512 The more or less narrow distribution pattern of these clades (Figs. 7, F–I) contrasts to a wide

513 distribution of the '*Drosanthemum* core clade' (Fig. 7, B– E), harbouring more widespread

514   lineages with more species potentially indicating broader overall-habitat preferences: clade IV

515   *Vespertina* (12 spp), clade II *Xamera* (8 spp) and the genetically and morphologically most

516   diverse clade I (*Drosanthemum* p.p.; ≥ 55 spp; Fig. 7). The bulk of species diversity has been

517   described in subgenus *Drosanthemum*, which falls in three subclades Ia–Ic not previously

518   recognized (Fig. 2). These three subclades show distinct distribution patterns, with Ia restricted

519   more or less to the fynbos area of GCFR, Ic extending far into the east and northeast, while Ib

520   extends north to 28° S (Fig. 7, B). Clade III, composed of species hitherto considered to belong

521   to subgenus *Drosanthemum*, shows the most diverse distribution of all clades, with a southern

522   group of poorly resolved species, and a lineage of several species extending to the northernmost

523   locality of *Drosanthemum*, the Brandberg in Namibia (Liede-Schumann, Meve & Grimm 2019;

524   Fig. 7, D).

525   Some more species-rich clades within *Drosanthemum* have also wide ecological preferences,

526   with representatives both at lower and higher elevations. Morphological adaptations to arid

527   habitats are capsules with deep pockets caused by false septa enabling seed retention (Hartmann

528   & Bruckmann 2000), which have been evolved in parallel in clade Ia and IIIb. However, whether

529   the possession of false septa in the capsules is restricted to species of arid habitats remains an

530   open question.

Conclusions

531

532   In this study, we present a comprehensive phylogenetic investigation of *Drosanthemum,* a

533   morphologically diverse genus that has so far been relatively overlooked in evolutionary studies

534   of Aizoaceae. Our results confirm *Drosanthemum* (= Drosanthemeae) as sister lineage to

535   Ruschieae, which is in accord with the 'core ruschioids' hypothesis (Klak, Reeves & Hedderson

536   2004; Klak, Bruyns & Hanáček 2013; Fig. 8). Additionally, our phylogenetic evidence signifies

537   *Drosanthemum* as a genetically well-structured but heterogenous lineage of mesomorphic plants

538   that is, however, less species-rich than its sister clade; a pattern of diversity distribution common

539   in the plant tree of life (Donoghue & Sanderson 2015). Still, our analysis suggest that

540   *Drosanthemum* is not simply a depauperate lineage sister to a radiation, but instead exemplifies a

541   radiation by itself as indicated by complex plastid and nuclear DNA sequence differentiation

542   patterns (Figs. 2, 3, 6), and the flower and fruit diversity present in the genus that is unusual for

543   Aizoaceae.

544 Occurrence patterns among the evolutionary lineages might further indicate geographic factors

545 playing a role in species diversification in *Drosanthemum*. While most of the evolutionary

546 history of the genus seem to have taken place in a relatively mesic environment in the

547 southwestern parts in the GCFR, several lineages apparently have started to adapt to more arid

548 and/or winter-cold areas. Genetically relictual species from at least two early radiations co-exist

549 among rapidly evolving lineages, reflecting species-delimitation problems in species-rich clades.

550 This is mirrored in the present study that largely supports the current taxonomic concepts in

551 *Drosanthemum* with few interesting exceptions, among others, cryptic species.

Acknowledgements

553 We (SLS and HEKH) thank the Mesemb Study Group (M.S.G.) for support from the Research

554 Fund in 2010 and 2013. Laco Mucina (Univ. of Western Australia) is thanked for a pleasant field

555 trip and a sample of *D. zygophylloides* and Hans-Dieter Ihlenfeldt (Univ. Hamburg) for

556 contributing several of the outgroup samples. SLS thanks the participants of the MSc Module F1

557 at the University of Bayreuth from 2008 to 2015 for their work on *Drosanthemum* herbarium

558 specimens. Angelika Täuber and Margit Gebauer (UBT) are thanked for their enduring and

559 conscientious lab work.

References

561 Banag CI, Mouly A, Alejandro GJD, Bremer B, Meve U, Grimm GW, Liede-Schumann S. 2017.

562 *Ixora* (Rubiaceae) on the Philippines – crossroad or cradle? *BMC Evolutionary Biology* 17:131

563 [e-pub]. DOI: https://doi.org/10.1186/s12862-017-0974-3.

564 Bandelt H-J, Forster P, Röhl A. 1999. Median-joining networks for inferring intraspecific

565 phylogenies. *Molecular Biology and Evolution* 16:37–48. DOI:

566 https://doi.org/10.1093/oxfordjournals.molbev.a026036.

567 Berger SA, Krompass D, Stamatakis A. 2011. Performance, accuracy, and web server for

568 evolutionary placement of short sequence reads under Maximum Likelihood. *Systematic Biology*

569 60:291–302. DOI: https://doi.org/10.1093/sysbio/syr010.

570 Bergsten, J. 2005, A review of long-branch attraction. *Cladistics*, 21:163–193. DOI:

571 https://doi.org/10.1111/j.1096-0031.2005.00059.x.

572   Bittrich V. 1990. Systematic studies in Aizoaceae. *Mitteilungen aus dem Institut für allgemeine*

573   *Botanik in Hamburg* 23b:491–508.

574   Bittrich V, Struck M. 1989. What is primitive in Mesembryanthemaceae? An analysis of

575   evolutionary polarity of character states. *South African Journal of Botany* 55: 321–331. DOI:

576   https://doi.org/10.1016/S0254-6299(16)31183-8.

577   Bohley K, Joos O, Hartmann HEK, Sage R, Liede-Schumann S, Kadereit G. 2015. Phylogeny of

578   Sesuvioideae (Aizoaceae)–Biogeography, leaf anatomy and the evolution of C 4 photosynthesis.

579   *Perspectives in Plant Ecology, Evolution and Systematics* 17:116–130. DOI:

580   https://doi.org/10.1016/j.ppees.2014.12.003.

581   Born J, Linder HP, Desmet PG. 2007. The greater cape floristic region. *Journal of Biogeography*

582   34:147–162. DOI: https://doi.org/10.1111/j.1365-2699.2006.01595.x.

583   Chesselet P, Smith GF, Van Wyk AE. 2002. A new tribal classification of

584   Mesembryanthemaceae: evidence from floral nectaries. *Taxon* 51:295–308. DOI:

585   https://doi.org/10.2307/1554899.

586   Chesselet P, Van Wyk AE, Smith GF. 2004. Notes on African plants: Mesembryanthemaceae. A

587   new tribe and adjustments to infrafamilial classification. *Bothalia - African Biodiversity &*

588   *Conservation* 34:47–47. DOI: https://doi.org/10.4102/abc.v34i1.412.

589   Denk T, Grimm GW. 2010. The oaks of western Eurasia: Traditional classifications and

590   evidence from two nuclear markers. *Taxon* 59:351–366. DOI:

591   https://doi.org/10.1002/tax.592002.

592   Donoghue MJ, Sanderson MJ. 2015. Confluence, synnovation, and depauperons in plant

593   diversification. *New Phytologist* 207: 260–274. DOI: https://doi.org/10.1111/nph.13367.

594   Ellis AG, Weis AE, Gaut BS. 2007. Spatial scale of local adaptation and population genetic

595   structure in a miniature succulent, *Argyroderma pearsonii*. *New Phytologist* 174:904–914. DOI:

596   https://doi.org/10.1111/j.1469-8137.2007.02043.x.

597   Felsenstein J. 2004. *Inferring Phylogenies*. Sunderland, MA, U.S.A.: Sinauer Associates Inc.

598 Fishbein M, Hibsch-Jetter C, Soltis DE, Hufford L. 2001. Phylogeny of Saxifragales

599 (Angiosperms, Eudicots): Analysis of a Rapid, Ancient Radiation. *Systematic Biology* 50: 817–

600 847. DOI: https://doi.org/10.1080/106351501753462821.

601 Graham SW, Iles WJD 2009. Different gymnosperm outgroups have (mostly) congruent signal

602 regarding the root of flowering plant phylogeny. *American Journal of Botany* 96: 216–227. DOI:

603 https://doi.org/10.3732/ajb.0800320.

604 Grimm GW, Renner SS, Stamatakis A, Hemleben V. 2006. A nuclear ribosomal DNA

605 phylogeny of *Acer* inferred with maximum likelihood, splits graphs, and motif analyses of 606

606 sequences. *Evolutionary Bioinformatics* 2:279–294. DOI:

607 https://doi.org/10.1177/117693430600200014.

608 Grímsson F, Grimm GW, Zetter R. 2018. Evolution of pollen morphology in Loranthaceae.

609 *Grana* 57:16–116. DOI: http://dx.doi.org/10.1080/00173134.2016.1261939.

610 Hartmann HEK. 1991. Mesembryanthema. *Contributions from the Bolus Herbarium* 13:75–157.

611 Hartmann HEK. 2006. Adaptations and phytogeography in the Ice-Plant family (Aizoaceae) - the

612 interaction of the genetic equipment and ecological parameters. II. Hide-and seek: plants sunk in

613 the ground. *Bradleya* 24:1–38. DOI: https://doi.org/10.25223/brad.n22.2004.a4.

614 Hartmann HEK. 2007. Studies in Aizoaceae: eight new subgenera in *Drosanthemum* Schwantes.

615 *Bradleya* 25:145–176. DOI: https://doi.org/10.25223/brad.n25.2007.a11.

616 Hartmann HEK. 2008. A carnival of flowers in *Drosanthemum* subgenus *Speciosa* (Aizoaceae).

617 *Bradleya* 26:99–120. DOI: https://doi.org/10.25223/brad.n26.2008.a7.

618 Hartmann HEK. 2016. Aizoaceae in North-East Africa: *Delosperma*. *Symbolae Botanicae*

619 *Upsalienses* 38:53–56. DOI: https://doi.org/10.25223/brad.n26.2008.a4.

620 Hartmann HEK. 2017a. *Aizoaceae A–G. Illustrated Handbook of Succulent Plants*, ed. 2. Berlin:

621 Springer Verlag, 658 pp.

622 Hartmann HEK. 2017b. *Aizoaceae H–Z. Illustrated Handbook of Succulent Plants*, ed. 2. Berlin:

623 Springer Verlag, 664 pp.

624 Hartmann HEK, Bruckmann C. 2000. The capsules of *Drosanthemum* Schwantes (Ruschioideae,

625 Aizoaceae). *Bradleya* 18:75–112. DOI: https://doi.org/10.25223/brad.n18.2000.a8.

626 Hartmann HEK, Le Roux A. 2011. *Drosanthemum* subgenus *Speciosa* (Aizoaceae): towards a

627 revision of the plants with black staminodes. *Bradleya* 29:143–178. DOI:

628 https://doi.org/10.25223/brad.n29.2011.a18.

629 Hartmann HEK, Liede-Schumann S. 2013. *Knersia* gen. nov., an emigrant from *Drosanthemum*

630 (Ruschieae, Ruschioideae, Aizoaceae). *Bradleya* 31:116–127. DOI:

631 https://doi.org/10.25223/brad.n31.2013.a14.

632 Hartmann HEK, Liede-Schumann S. 2014. Two new subgenera and one new species in the

633 genus *Drosanthemum*. *Bradleya* 32:50–63. DOI: https://doi.org/10.25223/brad.n32.2014.a19.

634 Hartmann HEK, Niesler IM. 2009. On the evolution of nectaries in Aizoaceae. *Bradleya* 27:69–

635 120. DOI: https://doi.org/10.25223/brad.n27.2009.a14.

636 Hassan NM, Thiede J, Liede-Schumann S. 2005. Phylogenetic analysis of Sesuvioideae

637 (Aizoaceae) inferred from nrDNA internal transcribed spacer (ITS) sequences and morphological

638 data. *Plant Systematics and Evolution* 255: 121–143. DOI: https://doi.org/10.1007/s00606-005-

639 0357-x.

640 Hennig W 1950. *Grundzüge einer Theorie der phylogenetischen Systematik*. Berlin: Deutscher

641 Zentralverlag.

642 Hijmans RJ, 2019. The raster package. *Available at https://rspatial.org/raster/pkg/index.html*

643 (accessed 5 August 2019).

644 Hijmans RJ, Cameron SE, Parra JL, Jones PG, Jarvis A. 2005. Very high resolution interpolated

645 climate surfaces for global land areas. *International Journal of Climatology* 25: 1965–1978.

646 Holland B, Moulton V. 2003. Consensus networks: A method for visualising incompatibilities in

647 collections of trees. In: Benson G, and Page R, eds. *Algorithms in Bioinformatics: Third*

648 *International Workshop, WABI, Budapest, Hungary Proceedings*. Berlin, Heidelberg, Stuttgart:

649 Springer Verlag, 165–176.

650 Hubert F, Grimm GW, Jousselin E, Berry V, Franc A, Kremer A. 2014. Multiple nuclear genes

651 stabilize the phylogenetic backbone of the genus *Quercus*. *Systematics and Biodiversity* 12:405–

652 423. DOI: https://doi.org/10.1080/14772000.2014.941037.

653 Huson DH, Bryant D. 2006. Application of phylogenetic networks in evolutionary studies.

654 *Molecular Biology and Evolution* 23:254–267. DOI: https://doi.org/10.1093/molbev/msj030.

655 Ihlenfeldt H-D. 1971. Some aspects of the biology of dissimination of the

656 Mesembryanthemaceae. In: Herre H, ed. *The Genera of Mesembryanthemaceae*. Cape Town:

657 Tafelberg-Uitgewers Beperk, 28–34.

658 Illing N, Klak C, Johnson C, Brito D, Negrao N, Baine F, van Kets V, Ramchurn KR, Seoighe C,

659 Roden L. 2009. Duplication of the Asymmetic Leaves1/Rough Sheath 2/Phantastica (ARP) gene

660 precedes the explosive radiation of the Ruschioideae. *Development, Genes, and Evolution*

661 219:331–338. DOI: https://doi.org/10.1007/s00427-009-0293-9.

662 Khanum R, Surveswaran S, Meve U, Liede-Schumann S. 2016. *Cynanchum* (Apocynaceae:

663 Asclepiadoideae): A pantropical Asclepiadoid genus revisited. *Taxon* 65:467–486. DOI:

664 http://dx.doi.org/10.12705/653.3.

665 Klak C, Bruyns PV. 2013. A new infrageneric classification for *Mesembryanthemum*

666 (Aizoaceae: Mesembryanthemoideae). *Bothalia* 43:197–206. DOI:

667 https://doi.org/10.4102/abc.v43i2.95.

668 Klak C, Bruyns PV, Hanáček P. 2013. A phylogenetic hypothesis for the recently diversified

669 Ruschieae (Aizoaceae) in southern Africa. *Molecular Phylogenetics and Evolution* 69:1005–

670 1020. DOI: https://doi.org/10.1016/j.ympev.2013.05.030.

671 Klak C, Bruyns PV, Hedderson TAJ. 2007. A phylogeny and new classification for

672 Mesembryanthemoideae. *Taxon* 56:737–756. DOI: https://doi.org/10.2307/25065857.

673 Klak C, Hanáček P, Bruyns PV. 2017a. Disentangling the Aizooideae: New generic concepts and

674 a new subfamily in Aizoaceae. *Taxon* 66:1147–1170. DOI: https://doi.org/10.12705/665.9.

675   Klak C, Hanáček P, Bruyns PV. 2017b. Out of southern Africa: Origin, biogeography and age of

676   the Aizooideae (Aizoaceae). *Molecular Phylogenetics and Evolution* 109:203–216. DOI:

677   https://doi.org/10.1016/j.ympev.2016.12.016.

678   Klak C, Hanáček P, Bruyns PV. 2018. A recircumscription of *Jacobsenia* (Aizoaceae): Re-

679   instating *Drosanthemopsis*, with two new quartz-endemics from Namaqualand, South Africa and

680   sinking *Knersia*. *South African Journal of Botany* 116:67–81. DOI:

681   https://doi.org/10.1016/j.sajb.2018.02.402.

682   Klak C, Khunou A, Reeves A, Hedderson TA. 2003. A phylogenetic hypothesis for the

683   Aizoaceae (Caryophyllales) based on four plastid DNA regions. *American Journal of Botany*

684   90:1433–1445. DOI: https://doi.org/10.3732/ajb.90.10.1433.

685   Klak C, Reeves G, Hedderson TA. 2004. Unmatched tempo of evolution in Southern African

686   semi-desert ice plants. *Nature* 427: 63–65. DOI: https://doi.org/10.1038/nature02243.

687   Landrum JV. 2001. Wide-band tracheids in leaves of genera in Aizoaceae: the systematic

688   occurrence of a novel cell type and its implications for the monophyly of the subfamily

689   Ruschioideae. *Plant Systematics and Evolution* 227:49–61. DOI:

690   https://doi.org/10.1007/s006060170056.

691   Liede-Schumann S, Newton LE. 2018. Notes on the *Delosperma* clade. *Haseltonia* 25:100–114.

692   DOI: https://doi.org/10.2985/026.025.0109.

693   Liede-Schumann S, Meve U, Grimm GW. 2019. New species in *Drosanthemum* (*Aizoaceae:*

694   *Ruschioideae*). *Bradleya* 37: 226–239. DOI: https://doi.org/10.25223/brad.n37.2019.a21.

695   Liede-Schumann S, Grimm GW, Nürk NM, Potts AJ, Meve U. 2019. Phylogenetic relationships

696   in the southern African genus *Drosanthemum* (Ruschioideae, Aizoaceae), v2, Dryad,

697   Dataset, https://doi.org/10.5061/dryad.n2z34tms2.

698   Maddison WP, Maddison DR. 2018. Mesquite: a modular system for evolutionary analysis.

699   Version 3.51. Available at: http://www.mesquiteproject.org.

700 Magallón S, Gómez-Acevedo SL, Sánchez-Reyes LL, Hernández-Hernández T. 2015. A

701 metacalibrated time-tree documents the early rise of flowering plant phylogenetic diversity. *New*

702 *Phytologist* 207:437–453. DOI: https://doi.org/10.1111/nph.13264.

703 Manning, JC, Goldblatt P. 2012. *Plants of the Greater Cape Floristic Region. 1: The Core Cape*

704 *Flora. Strelitzia* 29. Pretoria, South African National Biodiversity Institute.

705 Manos PS, Zhou ZK, Cannon CH. 2001. Systematics of Fagaceae: Phylogenetic tests of

706 reproductive trait evolution. *International Journal of Plant Sciences* 162:1361–1379. DOI:

707 https://doi.org/10.1086/322949.

708 Melo-de-Pinna GFA, Ogura AS, Arruda ECP, Klak C. 2014. Repeated evolution of endoscopic

709 peripheral vascular bundles in succulent leaves of Aizoaceae (Caryophyllales). *Taxon* 63:1037–

710 1052. https://dx.doi.org/10.12705/635.8

711 Mittermeier RA, Gil PR, Hoffmann M, Pilgrim J, Brooks T, Mittermeier CG, Lamoreux JF, Da

712 Fonseca GAB. 2004. *Hotspots revisited: Earth's Biologically Richest and Most Endangered*

713 *Terrestrial Ecoregions.* Chicago, Cemex & University of Chicago Press.

714 Mittermeier RA, Myers N, Thomsen JB, Da Fonseca GAB, Olivieri S. 1998. Biodiversity

715 hotspots and major tropical wilderness areas: approaches to setting conservation priorities.

716 *Conservation Biology* 12:516–520. DOI: https://doi.org/10.1046/j.1523-1739.1998.012003516.x.

717 Mittermeier RA, Turner WR, Larsen FW, Brooks TM, Gascon C. 2011. Global biodiversity

718 conservation: the critical role of hotspots. In: Zachos FE, Habel JC, eds. *Biodiversity hotspots*.

719 Berlin, Heidelberg, Springer Verlag, 3–22.

720 Morrison DA. 2010. Using data-display networks for exploratory data analysis in phylogenetic

721 studies. *Molecular Biology and Evolution* 27:1044–1057. DOI:

722 https://doi.org/10.1093/molbev/msp309.

723 Nürk NM, Madriñán S, Carine MA, Chase MW, Blattner FR. 2013. Molecular phylogenetics and

724 morphological evolution of St. John's wort (*Hypericum*; Hypericaceae). *Molecular Phylogenetics*

725 *and Evolution* 66:1–16. https://doi.org/10.1016/j.ympev.2012.08.022.

726   Nürk NM, Uribe-Convers S, Gehrke B, Tank DC, Blattner FR. 2015. Oligocene niche shift,

727   Miocene diversification – cold tolerance and accelerated speciation rates in the St. John's Worts

728   (*Hypericum*, Hypericaceae). *BMC Evolutionary Biology.* 15:80. DOI:

729   https://doi.org/10.1186/s12862-015-0359-4.

730   Oh S, Manos PS. 2008. Molecular phylogenetics and cupule evolution in Fagaceae as inferred

731   from nuclear *CRABS CLAW* sequences. *Taxon* 57:434–451. DOI:

732   https://doi.org/10.2307/25066014.

733   Paradis E. 2010. pegas: an R package for population genetics with an integrated-modular

734   approach. *Bioinformatics* 26:419–420. DOI: https://doi.org/10.1093/bioinformatics/btp696.

735   Parolin P. 2001. Seed expulsion in fruits of Mesembryanthema (Aizoaceae): a mechanistic

736   approach to study the effect of fruit morphological structures on seed dispersal. *Flora -*

737   *Morphology, Distribution, Fuctional Ecology of Plants* 196:313–322. DOI:

738   https://doi.org/10.1016/S0367-2530(17)30060-9.

739   Parolin P. 2006. Ombrohydrochory: Rain-operated seed dispersal in plants – With special regard

740   to jet-action dispersal in Aizoaceae. *Flora - Morphology, Distribution, Functional Ecology of*

741   *Plants* 201:511–518. DOI: https://doi.org/10.1016/j.flora.2005.11.003.

742   Pattengale ND, Masoud A, Bininda-Emonds ORP, Moret BME, Stamatakis A. 2009. How many

743   bootstrap replicates are necessary? In: Batzoglou S, ed. *RECOMB 2009*. Berlin, Heidelberg:

744   Springer-Verlag, 184–200.

745   Powell RF, Magee AR, Forest F, Cowan RS, Boatwright JS. 2019. A phylogeographic study of

746   the stoneplant *Conophytum* (Aizoaceae; Ruschioideae; Ruschieae) in the Bushmanland Inselberg

747   Region (South Africa) suggests anemochory. *Systematics and Biodiversity* 17:110–123. DOI:

748   https://doi.org/10.1080/14772000.2019.1571535.

749   Prescott A, Venning J. 1984. Aizoaceae. In Georg AS *Flora of Australia. Volume 4 —*

750   *Phytolaccaceae to Chenopodiaceae*. Canberra: Australian Government Publishing Service, 19–

751   62.

752   R Core Team 2019. R: A Language and Environment for Statistical Computing. R Foundation

753   for Statistical Computing, Vienna, Austria. https://www.R-project.org/ (accessed 17.11.2018).

754   Rust S, Bruckmann C, Hartmann HEK. 2002. The flowers of *Drosanthemum* Schwantes

755   (Ruschioideae, Aizoaceae). *Bradleya* 20:121–147. DOI:

756   https://doi.org/10.25223/brad.n20.2002.a13

757   Saarela JM, Rai HS, Doyle JA, Endress PK, Mathews S, Marchant AD, Briggs BG, Graham SW.

758   2007. Hydatellaceae identified as a new branch near the base of the angiosperm phylogenetic

759   tree. *Nature* 446: 312–315. DOI: https://doi.org/10.1038/nature05612.

760   Schliep K, Potts AJ, Morrison DA, Grimm GW. 2017. Intertwining phylogenetic trees and

761   networks. *Methods in Ecology and Evolution* 8: 1212–1220.DOI: https://doi.org/10.1111/2041-

762   210X.12760.

763   Schmiedel U, Jürgens N. 2004. Habitat ecology of southern African quartz fields: studies on the

764   thermal properties near the ground. *Plant Ecology* 170:153–166. DOI:

765   https://doi.org/10.1023/b:Vege.0000021661.56381.67.

766   Shaw J, Lickey EB, Schilling E, Small RL. 2007. Comparison of whole chloroplast genome

767   sequences to choose noncoding regions for phylogenetic studies in angiosperms: the tortoise and

768   the hare III. *American Journal of Botany* 94:275–288. DOI: https://doi.org/10.3732/ajb.94.3.275.

769   Simeone MC, Cardoni S, Piredda R, Imperatori F, Avishai M, Grimm GW, Denk, T. 2018.

770   Comparative systematics and phylogeography of *Quercus* Section *Cerris* in western Eurasia:

771   inferences from plastid and nuclear DNA variation. *PeerJ* 6:e5793. DOI:

772   https://doi.org/10.7717/peerj.5793.

773   Simeone MC, Grimm GW, Papini A, Vessella F, Cardoni S, Tordoni E, Piredda R, Franc A,

774   Denk T. 2016. Plastome data reveal multiple geographic origins of *Quercus* Group Ilex. *PeerJ*

775   4:e1897. DOI: https://doi.org/10.7717/peerj.1897.

776   Stamatakis A. 2006. Phylogenetic models of rate heterogeneity: A high performance computing

777   perspective. Proceedings of 20th IEEE/ACM International Parallel and Distributed Processing

778   Symposium (IPDPS2006), High Performance Computational Biology Workshop. Rhodos,

779   Greece, April 2006. p. [on CD, no page nos].

780   Stamatakis A. 2014. RAxML version 8: a tool for phylogenetic analysis and post-analysis of

781   large phylogenies. *Bioinformatics* 30:1312–1313. DOI:

782   https://doi.org/10.1093/bioinformatics/btu033.

783   Stevens PF (2001 onwards). Angiosperm Phylogeny Website. *Available at*

784   *http://www.mobot.org/MOBOT/research/APweb/* (accessed 08 July 2019).

785   Templeton AR, Crandall KA, Sing CF 1992. A cladistic analysis of phenotypic associations with

786   haplotypes inferred from restriction endonuclease mapping and DNA sequence data: III.

787   Cladogram estimation. *Genetics* 132: 619–633.

788   Thiede J. 2004. Phylogenetics, systematics and classification of the Aizoaceae: a reconsideration

789   based on molecular data. *Schumannia / Biodiversity and Ecology* 4:51–58.

790   Thiede J, Schmidt SA, Rudolph B. 2007. Phylogenetic implication of the chloroplast rpoC1

791   intron loss in the Aizoaceae (Caryophyllales). *Biochemical Systematics and Ecology* 35:372–

792   380. DOI: https://doi.org/10.1016/j.bse.2006.12.010.

793   Valente LM, Britton AW, Powell MP, Papadopulos AS, Burgoyne P, Savolainen V. 2014.

794   Correlates of hyperdiversity in southern African ice plants (Aizoaceae). *Botanical Journal of the*

795   *Linnean Society* 174:110–129. DOI: https://doi.org/10.1111/boj.12117.

796   Van Jaarsveld EJ. 2015. *Drosanthemum badspoortensis*, a new cliff-dwelling species from

797   Badspoort, Western-Cape, South Africa. Bradleya 33:128-135. DOI:

798   https://doi.org/10.25223/brad.n33.2015.a18.

799   Van Jaarsveld EJ. 2018. *Drosanthemum decumbens* (Aizoaceae), a new status for an obligatory

800   cremnophyte from the Western Cape, South Africa. Haseltonia 24:2–7. DOI:

801   https://doi.org/10.2985/026.024.0102.

802   Verboom GA, Archibald JK, Bakker FT, Bellstedt DU, Conrad F, Dreyer LL, Forest F, Galley

803   C, Goldblatt P, Henning JF, Mummenhoff K, Linder HP, Muasya AM, Oberlander KC,

804   Savolainen V, Snijman DA, Van der Niet T, Nowell TL. 2009. Origin and diversification of the

805   Greater Cape flora: Ancient species repository, hot-bed of recent radiation, or both? *Molecular*

806   *Phylogenetics and Evolution* 51:44–53. DOI: https://doi.org/10.1016/j.ympev.2008.01.037.

807   Vitelli M, Vessella F, Cardoni S, Pollegioni P, Denk T, Grimm GW, Simeone MC. 2017.

808   Phylogeographic structuring of plastome diversity in Mediterranean oaks (*Quercus* Group *Ilex*,

809   Fagaceae). *Tree Genetics & Genomes* 13:3. DOI: http://dx.doi.org/10.1007/s11295-016-1086-8.

810   Weigend M, Gottschling M, Hilger HH, Nürk NM. 2010. Five new species of *Lithospermum* L.

811   (Boraginaceae tribe Lithospermeae) in Andean South America: Another radiation in the

812   Amotape-Huancabamba Zone. *Taxon* 59:1161–1179. https://www.jstor.org/stable/20773985.

813   Wheeler TJ, Kececioglu JD. 2007. Multiple alignments by aligning alignments. *Bioinformatics*

814   *and Biology Insights* 23:i559–i568. DOI: http://dx.doi.org/10.1093/bioinformatics/btm226.

815

816

817 **Tables**

818 **Table 1 Infrafamilial classification of Aizoaceae**

819 **Table 2 Alignment and analysis parameters for the targeted sequence regions.** NLD,

820 number of literally duplicate (identical) sequences; PUC, proportion of undetermined matrix

821 cells ('gappyness'); DAP, number of distinct alignment patterns; NBS, number of necessary BS

822 pseudoreplicates; Approx. model, approximate of the DNA substitution model optimized by

823 RAxML for each gene region (in alphabetical order: A↔C, A↔G, A↔T, C↔G, C↔T, G↔T).

824 **Figures**

825 **Figure 1**: **Floral diversity in *Drosanthemum*.** A. *Drosanthemum lique* (subg. *Vespertina*, clade

826 IIIa; HH 34800, HBG); B. *Drosanthemum nordenstamii* (subg. *Drosanthemum*, clade Ia; HH

827 31525, HBG); C. *Drosanthemum papillatum* (subg. *Quastea*, clade VI; HH 32425, HBG); D.

828 *Drosanthemum cereale* (subg. *Speciosa*, clade Vb; HH 34489, HBG)—note the absence of black

829 staminodes; E. *Drosanthemum hallii* (subg. *Speciosa*; clade Vb; HH 34610, HBG)—note the

830 black staminodes; F. *Drosanthemum zygophylloides*. Photos A–E: H.E.K. Hartmann; F: L.

831 Mucina.

832 **Figure 2: Phylogeny of *Drosanthemum*.** ML tree inferred by partitioned analysis of the cpDNA

833 sequence data. Edge lengths are drawn proportionally to the expected number of substitutions.

834 The nine main clades are annotated by roman numbers I–IX and coloured branches, with ML

835 bootstrap support indicated by edge width (values given for the nine main clades). Bars and

836 names to the right indicate subgeneric classification *sensu* Hartmann 2007. An asterisk after tip

837 names indicate accessions with literally duplicate sequences. CU, clade unique ITS mutation

838 pattern(s); Sh, shared ITS mutation pattern found occasionally also in other clades. Rooting is

839 according to the most likely position inferred by outgroup-EPA (scenario 1; outgroups removed).

840 **Figure 3: Bootstrap consensus network of *Drosanthemum*.** Consensus network based on 600

841 pseudoreplicate samples inferred by partitioned ML analysis of the cpDNA sequence data. Edge

842 lengths are proportional to the frequency of the phylogenetic split in the pseudoreplicate sample.

843 Branch colours and labels are as in Fig. 3. Black arrows indicate potential root positions inferred

844   by outgroup-EPA, with arrow size proportional to the probability estimate p_R (supplemental

845   information S4: Table S4).

846   **Figure 4: Median-joining networks of *Drosanthemum* clades I-IV.** Collapsed Median

847   networks; collapsed network portions (haplotype groups) represented by by circles; letters in

848   bold refer to Liede-Schumann et al. 2019 (file Haplotyping.xlsx; archive includes full networks).

849   Circle size does not show haplotype frequency but gives the maximum number of mutations

850   between grouped haplotypes/ connective medians (a group's dimension); edge length (minimum)

851   number of mutations between haplotype groups (Grimm 2019). A–D. Clade I. Note that subclade

852   Ib is paraphyletic to clades Ia and Ic according to *rpl*16 intron, *trn*K-*rps*16 and *rps*16-*trn*Q.

853   Filled black circles (medians) denote position of the consensus sequence of the clade. E–H.

854   Clades III and IV. Note that clade IIIa bridges between haplotype groups diagnostic for clades

855   IIIb and IV, which could be an indication of paraphyly (clade IIIa species originate from a

856   radiation predating the formation and subsequent radiation of clades IIIb and IV).

857   **Figure 5: Median-joining networks of *Drosanthemum* clades V–IX**. Collapsed Median

858   networks; collapsed network portions (haplotype groups) represented by circles; letters in bold

859   refer to Liede-Schumann et al. 2019 (file Haplotyping.xlsx; archive includes full networks).

860   Circle size does not show haplotype frequency but gives the maximum number of mutations

861   between grouped haplotypes/ connective medians (a group's dimension); edge length (minimum)

862   number of mutations between haplotype groups (Grimm 2019). A–D. Clades V and VI. Note the

863   central (*trn*S-*trn*G) or ancestral (*rps*16-*trn*Q) position of *D. gracillimum* (no *rpl*16 and *trn*K–

864   *rps*16 data available). E–H. Clades VII–IX. Note that members of each clade are clearly

865   differentiated but differ in the level of derivation per gene region.

866   **Figure 6**: **Statistical parsimony network of *Drosanthemum* ITS genotypes.** Network inferred

867   by analysis of the ITS sequence data under an infinite site model. Genotypes are indicated by

868   circles coloured according to clades inferred by cpDNA sequence analysis (see Figs. 3, 4). Circle

869   size indicate absolute frequency of genotypes (see legend). Black lines indicate steps in the

870   network, filled black circles missing genotypes, and dashed grey lines alternative links.

871   Genotypes in the centre of the graph are ancestral, those in the periphery most derived. Genotype

872   4 represents the genus consensus sequence found in several accessions of clade I (for details see

873   supplemental information S3).

874   **Figure 7**: **Distribution of *Drosanthemum***. A. Overall distribution of *Drosanthemum* in Africa.

875   B–J. Clade-wise distribution of *Drosanthemum* species in southern Africa. Filled symbols

876   indicate accessions used in the phylogeny, empty symbols indicate the remaining accessions in

877   the occurrence dataset of *Drosanthemum*. *D. zygophyl*., *D. zygophylloides*. Maps were created

878   using the elevation above sea level data from the WorldClim climate layers (Hijmans et al.,

879   2005), with a spatial resolution of 30' using the RASTER library v2.8-19 (Hijmans 2019) in R

880   v3.5.3 (R Core Team, 2019).

881   **Figure 8**: **Phylogeny of Aizoaceae**. A summary cladogram indicating recognized subfamilies

882   (*sensu* Klak, Hanáček & Bruyns 2017a) and tribes (*sensu* Chesselet, Van Wyk & Smith 2004)

883   detailing the number of genera and species and estimated node ages. Superscript letters denote

884   reference: *a*, Klak & Bruyns 2013; *b*, Hartmann 2017a; Hartmann 2017b; *c*, Stevens, 2001

885   onwards; *d*, Klak, Bruyns & Hanáček 2013; *e*, Klak, Hanáček & Bruyns 2017b; *f*, Valente et al.

886   2014; *g*, Magallón et al. 2015. A superscript asterisk denotes ages according to Klak, Hanáček &

887   Bruyns 2017a: Fig. S2.

888

Online supporting material

890   **Supplemental Information S1** [PDF]: Voucher table, indicating botanical name, voucher and

891   ENA number of the sequences used.

892   **Supplemental Information S2** [PDF]: Examples of character re-coding used for intra-clade

893   haplotype analyses (Figures S2A–C).

894   **Supplemental Information S3** [HTML]: Results of the statistical parsimony (SP) network

895   analyses of ITS sequence variation including genotype assignment and subclade networks.

896   **Supplemental Information S4** [PDF]: Results of outgroup-EPA detailing the five most

897   probable root positions in *Drosanthemum* (Figs. S4.2–6), and the probability of all query

898   placements (Table S4). Also including the result of the phylogenetic ML analysis of the

899   "Ruschioideae" cpDNA data (Fig. S4.1).

900

Infrafamilial classification of Aizoaceae

Subfamilies	Tribes
Sesuvioideae Lindl.	
Aizooideae Arn.	
Acrosanthoideae Klak	
Mesembryanthemoideae Ihlenf., Schwantes & Straka	
	Apatesieae Schwantes ex Ihlenf., Schwantes & Straka
	Dorotheantheae (Schwantes ex Ihlenf. & Struck) Chess., Gideon F. Sm. & A.E. van Wyk
Ruschioideae Schwantes	**Drosanthemeae** Chess., Gideon F. Sm. & A.E. van Wyk
	Ruschieae Schwantes ex Ihlenf., Schwantes & Straka

"Mesembs"

"core ruschioids"

Alignment and analysis parameters for the targeted sequence regions

NLD, number of literally duplicate (identical) sequences; PUC, proportion of undetermined matrix cells ('gappyness'); DAP, number of distinct alignment patterns; NBS, number of necessary BS pseudoreplicates; Approx. model, approximate of the DNA substitution model optimized by RAxML for each gene region (in alphabetical order: A↔C, A↔G, A↔T, C↔G, C↔T, G↔T).

Gene region	Matrix dimension (OTU × characters)	NLD	PUC	DAP	NBS	Approx. model
ITS	112 × 440[a]	27	2.7%	130	500	aabcde
trnS-trnG	121 × 1157	34	30.8%	305	800	aabbba
rpl16 intron	112 × 1193	36	22.0%	201	450	aabaaa
trnK-rps16	122 × 768	31	20.6%	241	450	aabccc
rps16-trnQ	127 × 788[b]	19	21.8%	245	550	aababa

[a] Only ITS1 and ITS2, flanking rRNA and 5.8S rRNA genes not included.

[b] After exclusion of the 'high-div' region.

Figure 1

Floral diversity in *Drosanthemum*

A. *Drosanthemum lique* (subg. *Vespertina*, clade IIIa; HH 34800, HBG); B. *Drosanthemum nordenstamii* (subg. *Drosanthemum*, clade Ia; HH 31525, HBG); C. *Drosanthemum papillatum* (subg. Quastea, clade VI; HH 32425, HBG); D. *Drosanthemum cereale* (subg. *Speciosa*, clade Vb; HH 34489, HBG)—note the absence of black staminodes; E. *Drosanthemum hallii* (subg. *Speciosa*; clade Vb; HH 34610, HBG)—note the black staminodes; F. *Drosanthemum zygophylloides*. Photos A−E: H.E.K. Hartmann; F: L. Mucina.

Figure 2

Phylogeny of *Drosanthemum*

ML tree inferred by partitioned analysis of the cpDNA sequence data. Edge lengths are scaled on expected number of substitutions. The nine main clades are annotated by roman numbers I–IX and coloured branches, with ML bootstrap support indicated by edge width (values given for the nine main clades). Bars and names to the right indicate subgeneric classification *sensu* Hartmann 2007. An asterisk after tip names indicate accessions with literally duplicate sequences. CU, clade unique ITS mutation pattern(s); Sh, shared ITS mutation pattern found occasionally also in other clades. Rooting is according to the most likely position inferred by outgroup-EPA (scenario 1; outgroups removed)

Nuclear ITS genotypes
(not included during tree inference)

★ Species with genus-consensus ITS

★ Species with ITS deviating by a single
mutation from the genus-consensus

★ Least derived V-type ITS, one consistent
transversion to genus consensus

Bootstrap support

75 — 89.9

90 — 100

Ic

Ia

I 69

(Ib)

subg.
Drosanthemum

D. hispidum HH 33866
D. hispidum HH 34262
D. floribundum HH 34403
D. candens HH 31897
D. candens HH 25014
D. spec. HH 30568
D. spec. HH 32382
D. candens HH 30541
D. dejagerae HH 31812   [*Xamera*]
D. spec. HH 33182
D. tuberculiferum HH 32398
D. prostratum HH 34592
D. prostratum aff HH 34316
D. archeri HH 31788
D. archeri HH 31774
D. glabrescens HH 32256
D. muirii HH 32209
D. ambiguum HH 30388
D. opacum HH 32212
D. spec. HH 25365
D. spec. HH 34496
D. spec. HH 32392neu
D. spec. Mucina 161005_14
D. intermedium HH 32200
D. intermedium HH 32439
D. spec. HH 34472
D. spec. HH 25376
D. framesii HH 32339
D. muirii HH 30321
D. subplanum HH 32259
D. oculatum HH 31710
D. schoenlandianum Bruyns 7172
D. oculatum HH 31680
D. schoenlandianum HH 25751
D. latipetalum HH 31568
D. latipetalum HH 31605
D. nordenstamii HH 31533
D. latipetalum HH 32217
D. spec. HH 32218
D. marinum HH 32205

II 77
1 CU, 1 Sh

subg.
Xamera

D. fourcadei HH 33900
D. dipageae HH 34409
D. spec. HH 34424
D. spec. HH 34586
D. delicatulum HH 30782   [*Drosanthemum*]
D. delicatulum HH 32462
D. curtophyllum HH 32673
D. subclausum HH 25737   [*Drosanthemum*]
D. praecultum HH 31824

III
IIIb
75

(IIIa)

subg.
Drosanthemum

D. obibense HH 25979
D. obibense HH 25972
D. luederitzii HH 26095
D. nollothense HH 31547, HH31569*
D. brevifolium HH 32242
D. ramosissimum US110492
D. cymiferum HH 25811   [*Quastea*]
D. cymiferum HH 31686
D. acutifolium HH 32406
D. erigeriflorum HH 26196
D. parvifolium HH 30399

IV
99
2–3 CU, 2 Sh

subg.
Vespertina

D. spec. HH 25424
D. spec. HH 33490
D. spec. HH 31925
D. spec. HH 31059
D. spec. HH 26170a
D. crassum HH 25896
D. spec. HH 32404
D. albiflorum HH 32383
D. lique HH 34447
D. spec. HH 34804
D. spec. HH 32378

Va

V 82

Vb

3 (–4) CU, 1 Sh

subg.
Speciosa

D. micans LeRoux 83_2
D. micans HH 34597
D. boerharvii HH 34596
D. hallii HH 34610
D. boerharvii HH 34478
D. speciosum HH 34619
D. pulchrum HH 34712
D. speciosum Bruyns 9006
D. chrysum HH 34631
D. austricola HH 34695   [*Ossicula*]   *D. boerharvii* HH 34697*, *D. lavisii* HH 34693*
D. flavum HH 34706
D. cereale HH 34492
D. cereale HH 34491
D. cereale HH 34490
D. flammeum HH 34460
D. brakfonteinense HH 34688
D. edwardsiae HH 34648
D. edwardsiae HH 34651
D. uniondalense HH 34813
D. boerharvii HH 34480
D. gracillimum Bruyns 7170   [*Vespertina*]

subg.
Ossicula

D. attenuatum HH 11826
D. attenuatum aff HH 34650
D. hispifolium HH 34587
D. hispifolium HH 32206
D. pallens Bayer 7454
D. striatum HH 29013
D. striatum HH 34698
D. spec. HH 34699   // reduced by factor 2   *D. striatum* HH 34720

VI
91
3 Sh

subg.
Necopina

D. acuminatum HH 34608
D. ecclesianum HH 34814
D. ecclesianum HH 34815
D. semiglobosum HH 34593
D. thudichumii HH 34714
D. bicolor HH 32459

VII 97

subg.
Quastea

D. papillatum HH 34614
D. papillatum HH 34607
D. papillatum HH 34624
D. papillatum HH 34629
D. calycinum HH 32211
D. papillatum HH 34456
D. expersum HH 34598
D. expersum HH 34590
D. cymiferum HH 32250

IX
98
2 Sh

D. longipes Bruyns 6037   [*Decidua*]
D. longipes van Jaarsveld s.n.
D. decidum HH 32241
D. deciduum Klak 1638
D. anemophilum van Jaarsveld s.n.
D. inornatum HH 32654
D. inornatum Bruyns 10066

D. longipes

subg.
Decidua

VIII 99
1 CU, 1 Sh

subg.
Quadrata

D. asperulum Bruyns 9005
D. tetramerum HH 34488
D. asperulum HH 34502
D. quadratum Bruyns 7812
D. quadratum HH 34503

D. zygophylloides

D. zygophylloides Mucina 130216_4
D. zygophylloides Klak 830

0.001

Figure 3

Bootstrap consensus network of *Drosanthemum*

Consensus network based on 600 pseudoreplicate samples inferred by partitioned ML analysis of the cpDNA sequence data. Edge lengths are proportional to the frequency of the phylogenetic split in the pseudoreplicate sample. Branch colours and labels are as in Fig. 3. Black arrows indicate potential root positions inferred by outgroup-EPA, with arrow size proportional to the probability estimate p_R (supplementary information S4, Table S4).
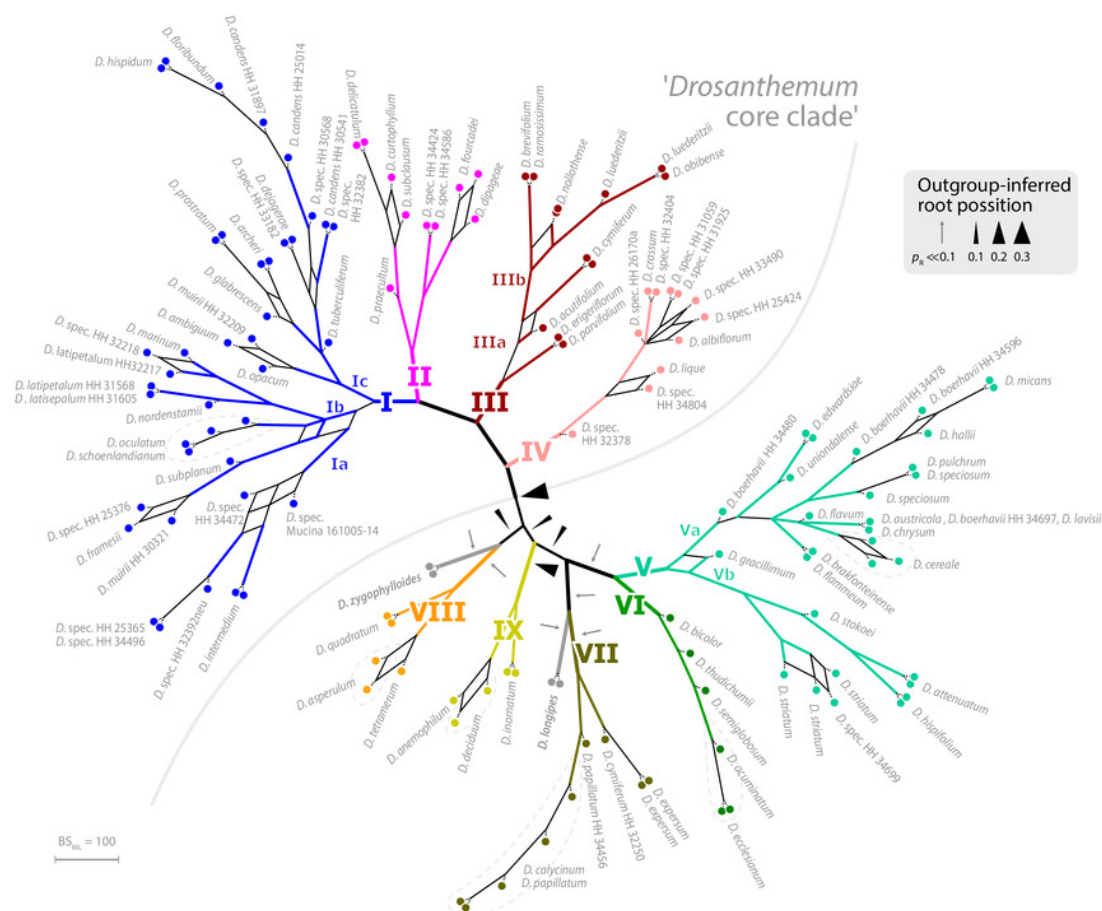
Figure 4

Median-joining networks of *Drosanthemum* clades I-IV

Collapsed Median networks; collapsed network portions (haplotype groups) represented by by circles; letters in bold refer to Liede-Schumann et al. 2019 (file Haplotyping.xlsx; archive includes full networks). Circle size does not show haplotype frequency but gives the maximum number of mutations between grouped haplotypes/ connective medians (a group's dimension); edge length (minimum) number of mutations between haplotype groups (Grimm 2019). A–D. Clade I. Note that subclade Ib is paraphyletic to clades Ia and Ic according to *rpl*16 intron, *trn*K-*rps*16 and *rps*16-*trn*Q. Filled black circles (medians) denote position of the consensus sequence of the clade. E–H. Clades III and IV. Note that clade IIIa bridges between haplotype groups diagnostic for clades IIIb and IV, which could be an indication of paraphyly (clade IIIa species originate from a radiation predating the formation and subsequent radiation of clades IIIb and IV).
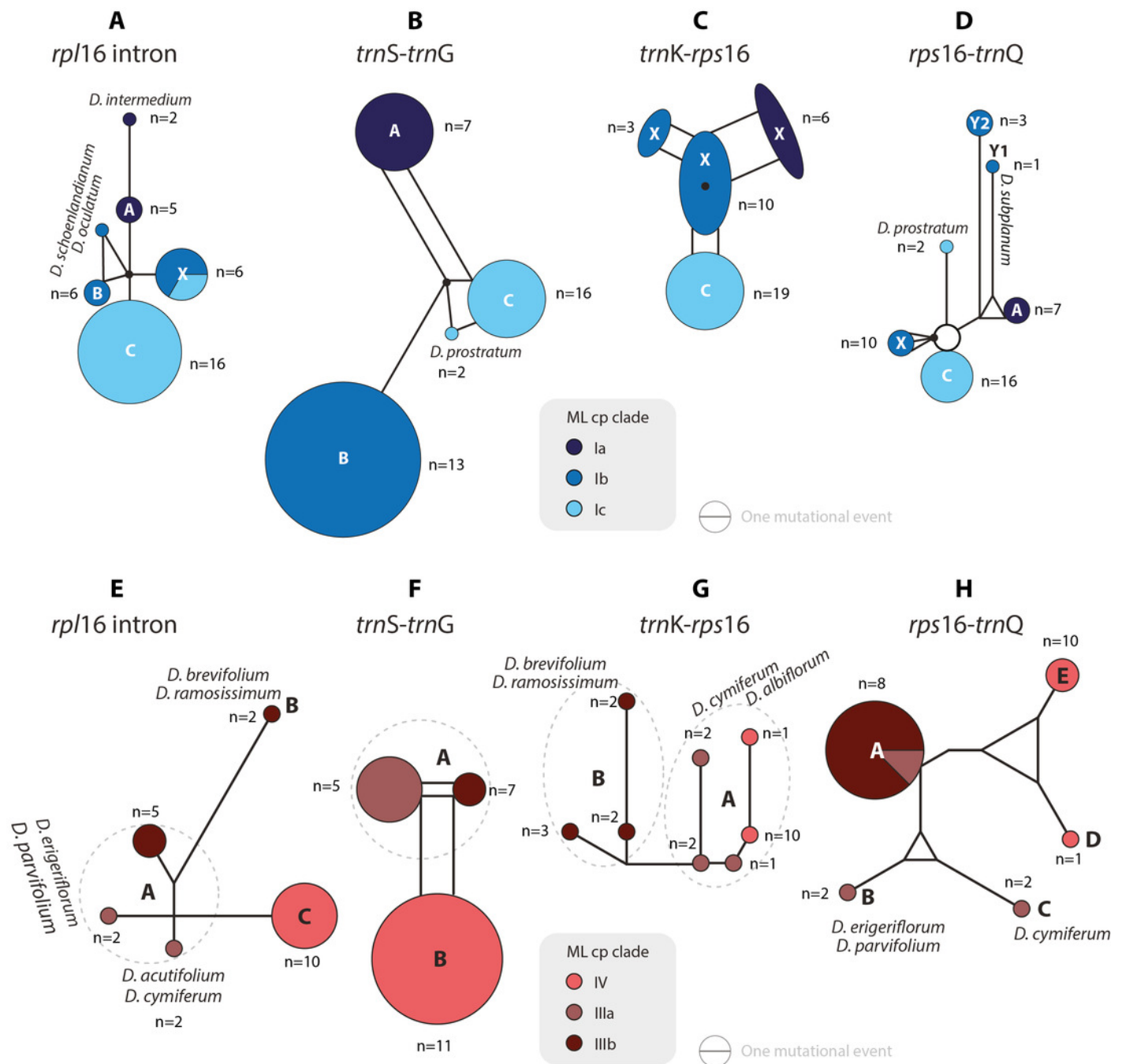
A
*rpl*16 intron

D. intermedium
n=2

D. schoenlandianum
D. oculatum

A n=5

X n=6

B n=6

C n=16

B
trnS-trnG

A n=7

C n=16

D. prostratum
n=2

B n=13

C
*trnK-rps*16

X n=3

X n=6

X n=10

C n=19

D
*rps*16-*trn*Q

Y2 n=3

Y1 n=1

D. subplanum

D. prostratum
n=2

A n=7

X n=10

C n=16

ML cp clade
- Ia
- Ib
- Ic

One mutational event

E
*rpl*16 intron

D. brevifolium
D. ramosissimum
B n=2

n=5

D. erigeriflorum
D. parvifolium

A

n=2

C n=10

D. acutifolium
D. cymiferum
n=2

F
trnS-trnG

n=5

A n=7

B n=11

G
*trnK-rps*16

D. brevifolium
D. ramosissimum
n=2

D. cymiferum
D. albiflorum

n=2

n=1

B

n=2

n=3

A

n=2

n=10

n=1

H
*rps*16-*trn*Q

n=10

n=8

A

E

D n=1

B n=2

D. erigeriflorum
D. parvifolium

n=2

C

D. cymiferum

ML cp clade
- IV
- IIIa
- IIIb

One mutational event

Figure 5

Median-joining networks of *Drosanthemum* clades V–IX

Collapsed Median networks; collapsed network portions (haplotype groups) represented by circles; letters in bold refer to Liede-Schumann et al. 2019 (file Haplotyping.xlsx; archive includes full networks). Circle size does not show haplotype frequency but gives the maximum number of mutations between grouped haplotypes/ connective medians (a group's dimension); edge length (minimum) number of mutations between haplotype groups (Grimm 2019). A–D. Clades V and VI. Note the central (*trn*S-*trn*G) or ancestral (*rps*16-*trn*Q) position of *D. gracillimum* (no *rpl*16 and *trn*K–*rps*16 data available). E–H. Clades VII–IX. Note that members of each clade are clearly differentiated but differ in the level of derivation per gene region.
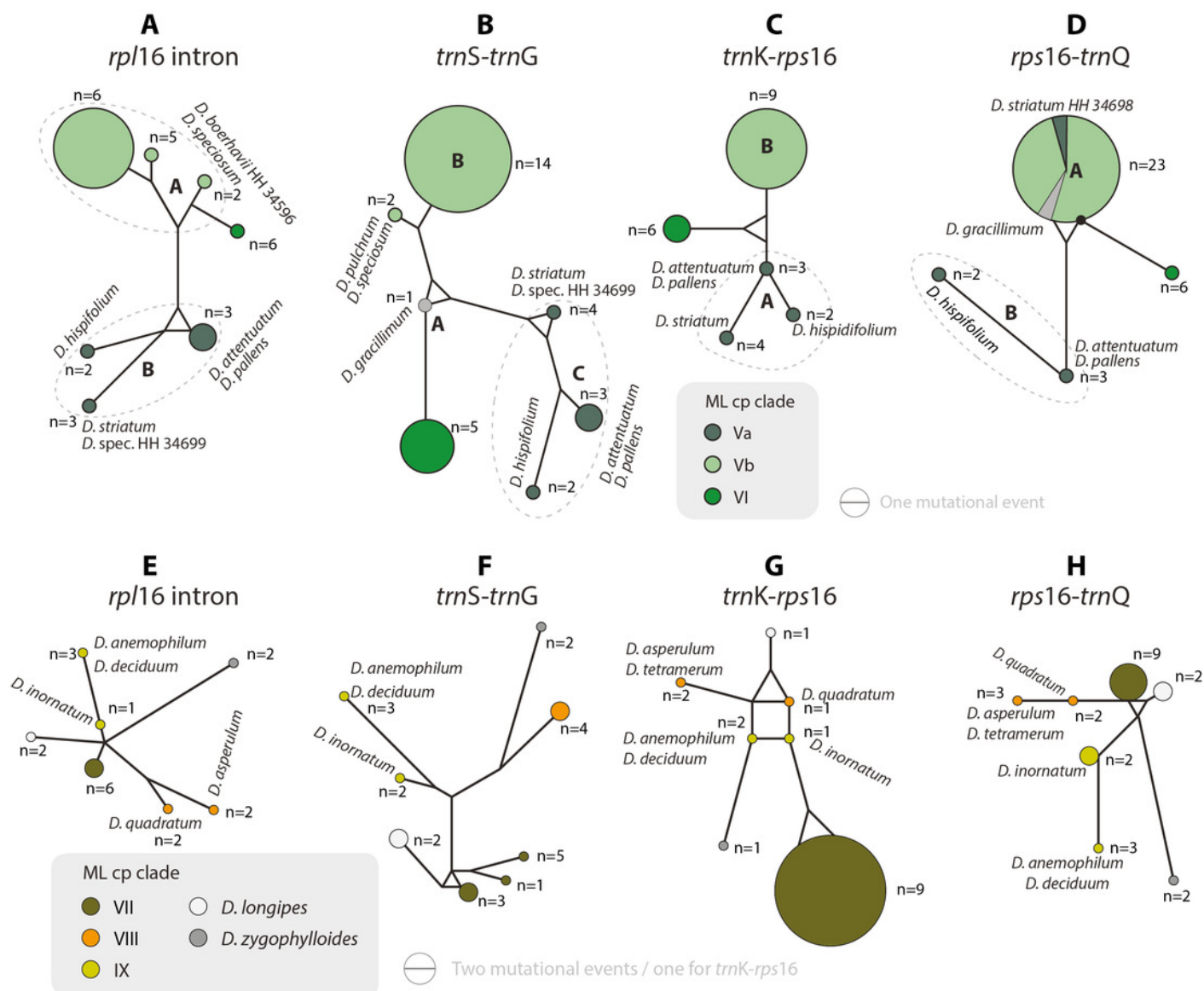
Figure 6

Statistical parsimony network of *Drosanthemum* ITS genotypes

Network inferred by analysis of the ITS sequence data under an infinite site model. Genotypes are indicated by circles coloured according to clades inferred by cpDNA sequence analysis (see Figs. 3, 4). Circle size indicate absolute frequency of genotypes (see legend). Black lines indicate steps in the network, filled black circles missing genotypes, and dashed grey lines alternative links. Genotypes in the centre of the graph are ancestral, those in the periphery most derived. Genotype 4 represents the genus consensus sequence found in several accessions of clade I (for details see supplementary information S3).
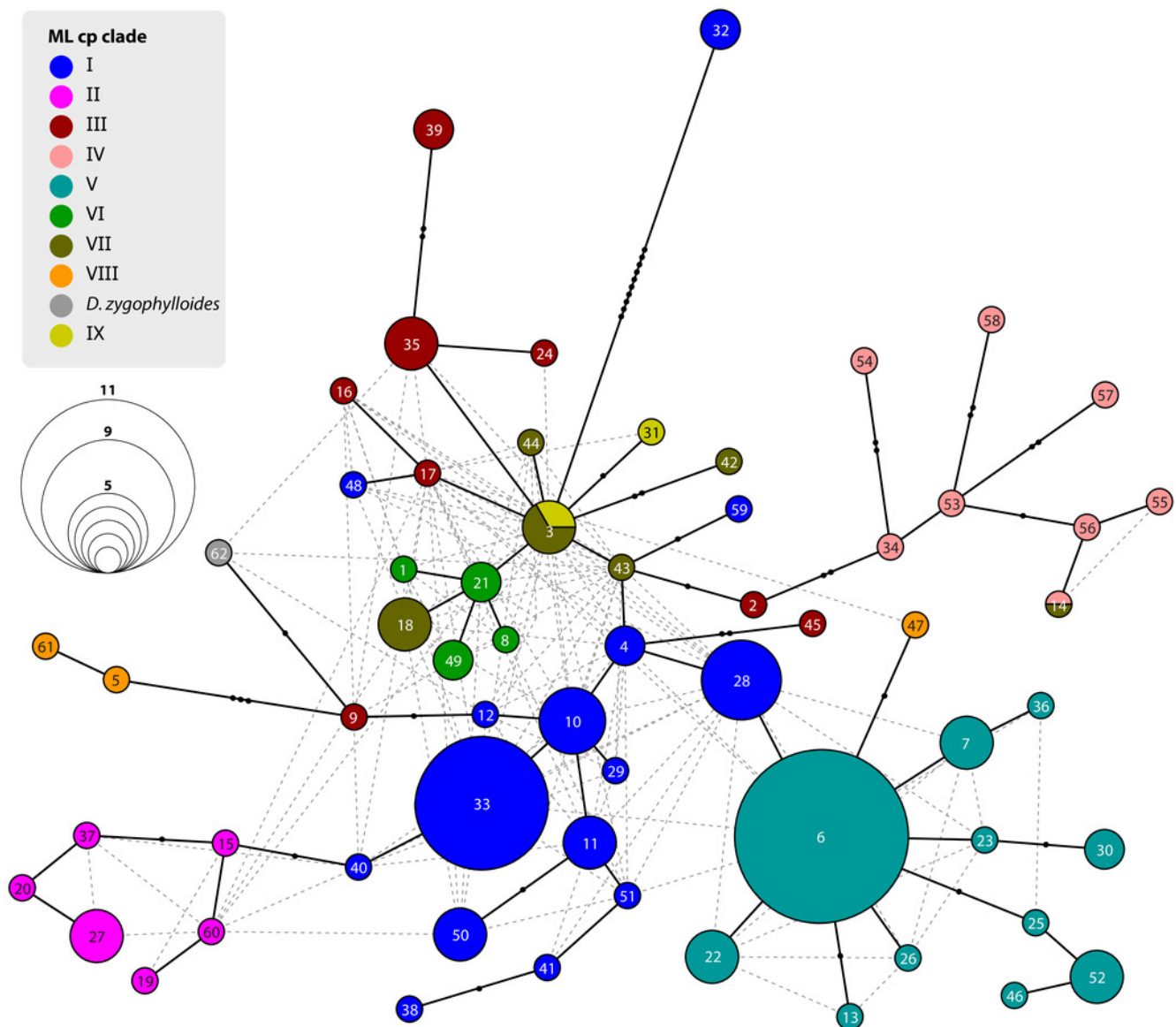
Figure 7

Distribution of *Drosanthemum*

A. Overall distribution of *Drosanthemum* in Africa. B–J. Clade-wise distribution of *Drosanthemum* species in southern Africa. Filled symbols indicate accessions used in the phylogeny, empty symbols indicate the remaining accessions in the occurrence dataset of *Drosanthemum*. *D.zygophyl.*, *D.zygophylloides*. Maps were created using the elevation above sea level data from the WorldClim climate layers (Hijmans et al., 2005), with a spatial resolution of 30' using the raster library v2.8-19 (Hijmans 2019) in R v3.5.3 (R Core Team, 2019).
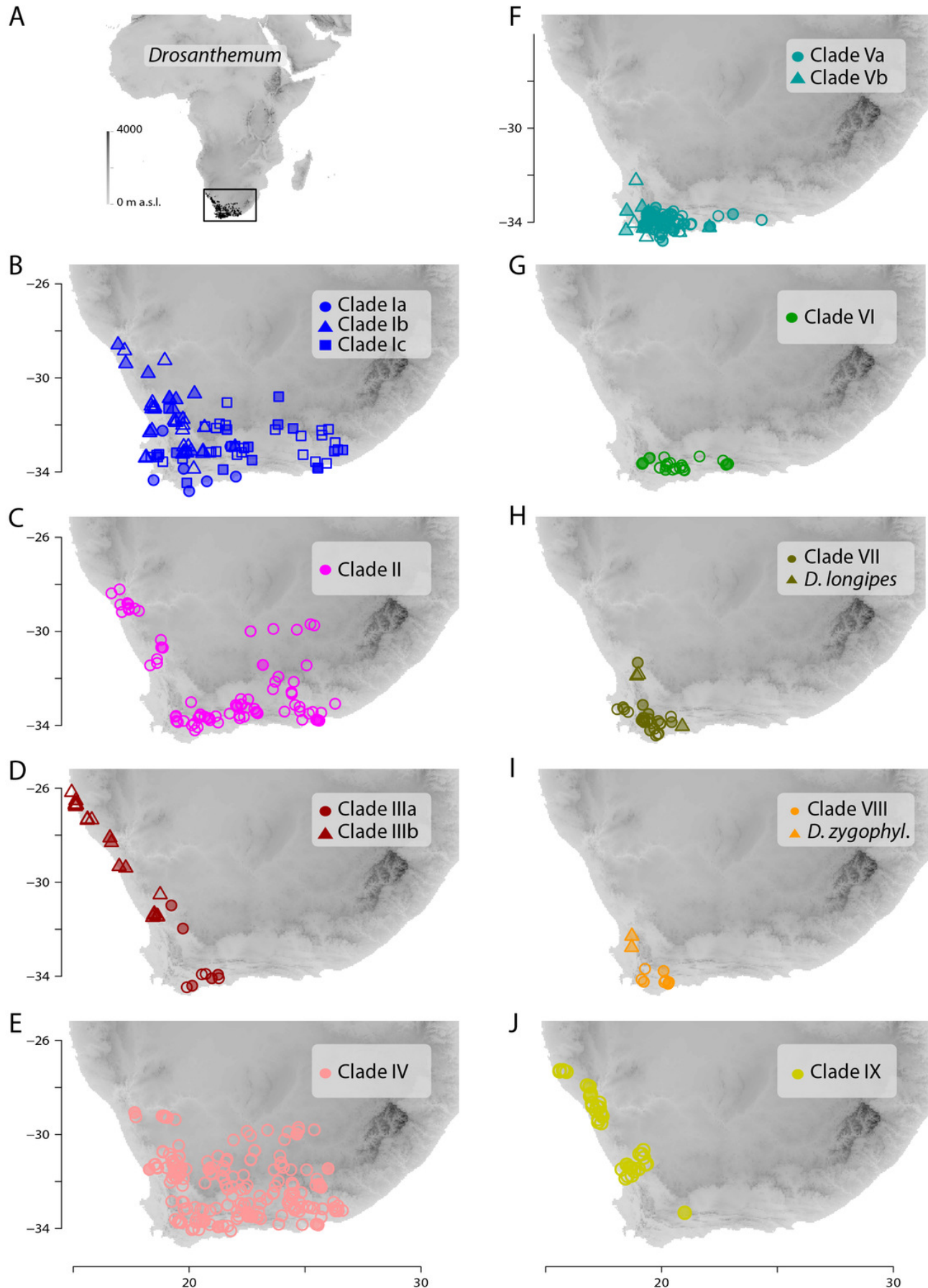
Figure 8

Phylogeny of Aizoaceae

A summary cladogram indicating recognized subfamilies (*sensu* Klak, Hanáček & Bruyns 2017a) and tribes (*sensu* Chesselet, Van Wyk & Smith 2004) detailing the number of genera and species and estimated node ages. Superscript letters denote reference: *a*, Klak & Bruyns 2013; *b*, Hartmann 2017a; Hartmann 2017b; *c*, Stevens, 2001 onwards; *d*, Klak, Bruyns & Hanáček 2013; *e*, Klak, Hanáček & Bruyns 2017b; *f*, Valente et al. 2014; *g*, Magallón et al. 2015. A superscript asterisk denotes ages according to Klak, Hanáček & Bruyns 2017a, Fig. S2.